Brain Stimulation 16 (2023) 567–593

Contents lists available at ScienceDirect

Brain Stimulation

journal homepage: http://www.journals.elsevier.com/brain-stimulation

TMS combined with EEG: Recommendations and open issues for data collection and analysis

Julio C. Hernandez-Pavon [a, b, c, 1, *], Domenica Veniero [d, 1, **], Til Ole Bergmann [e, f], Paolo Belardinelli [g, h], Marta Bortoletto [i], Silvia Casarotto [j, k], Elias P. Casula [l], Faranak Farzan [m], Matteo Fecchio [n], Petro Julkunen [o, af], Elisa Kallioniemi [p], Pantelis Lioumis [q, r], Johanna Metsomaa [q, r], Carlo Miniussi [g], Tuomas P. Mutanen [q, r], Lorenzo Rocchi [s, t], Nigel C. Rogasch [u, v, w], Mouhsin M. Shafi [x], Hartwig R. Siebner [y, z, aa], Gregor Thut [ab], Christoph Zrenner [h, ac, ad, ae], Ulf Ziemann [h, ad], Risto J. Ilmoniemi [q, r]

[a] Department of Physical Medicine and Rehabilitation, Feinberg School of Medicine, Northwestern University, Chicago, IL, USA
[b] Legs + Walking Lab, Shirley Ryan AbilityLab, Chicago, IL, USA
[c] Center for Brain Stimulation, Shirley Ryan AbilityLab, Chicago, IL, USA
[d] School of Psychology, University of Nottingham, UK
[e] Neuroimaging Center (NIC), Focus Program Translational Neuroscience (FTN), Johannes Gutenberg University Medical Center, Germany
[f] Leibniz Institute for Resilience Research (LIR), Mainz, Germany
[g] Center for Mind/Brain Sciences - CIMeC, University of Trento, Rovereto, TN, Italy
[h] Department of Neurology & Stroke, University of Tübingen, Tübingen, Germany
[i] Neurophysiology Lab, IRCCS Istituto Centro San Giovanni di Dio Fatebenefratelli, Brescia, Italy
[j] Department of Biomedical and Clinical Sciences, University of Milan, Milan, Italy
[k] IRCCS Fondazione Don Carlo Gnocchi ONLUS, Milan, Italy
[l] Department of Systems Medicine, University of Tor Vergata, Rome, Italy
[m] Simon Fraser University, School of Mechatronic Systems Engineering, Surrey, British Columbia, Canada
[n] Center for Neurotechnology and Neurorecovery, Department of Neurology, Massachusetts General Hospital, Boston, MA, USA
[o] Department of Technical Physics, University of Eastern Finland, Kuopio, Finland
[p] Department of Biomedical Engineering, New Jersey Institute of Technology, Newark, NJ, USA
[q] Department of Neuroscience and Biomedical Engineering, Aalto University, Espoo, Finland
[r] BioMag Laboratory, HUS Medical Imaging Center, Helsinki University Hospital, Helsinki University and Aalto University School of Science, Helsinki, Finland
[s] Department of Clinical and Movement Neurosciences, UCL Queen Square Institute of Neurology, University College London, London, United Kingdom
[t] Department of Medical Sciences and Public Health, University of Cagliari, Cagliari, Italy
[u] University of Adelaide, Adelaide, Australia
[v] South Australian Health and Medical Research Institute, Adelaide, Australia
[w] Monash University, Melbourne, Australia
[x] Berenson-Allen Center for Noninvasive Brain Stimulation, Department of Neurology, Beth Israel Deaconess Medical Center, Harvard Medical School, Boston, MA, USA
[y] Danish Research Centre for Magnetic Resonance, Centre for Functional and Diagnostic Imaging and Research, Copenhagen University Hospital - Amager and Hvidovre, Copenhagen, Denmark
[z] Department of Neurology, Copenhagen University Hospital Bispebjerg and Frederiksberg, Copenhagen, Denmark
[aa] Department of Clinical Medicine, Faculty of Health and Medical Sciences, University of Copenhagen, Copenhagen, Denmark
[ab] School of Psychology and Neuroscience, University of Glasgow, United Kingdom
[ac] Temerty Centre for Therapeutic Brain Intervention, Centre for Addiction and Mental Health, Toronto, Canada
[ad] Hertie Institute for Clinical Brain Research, University of Tübingen, Tübingen, Germany
[ae] Department of Psychiatry, University of Toronto, Toronto, Canada
[af] Department of Clinical Neurophysiology, Kuopio University Hospital, Kuopio, Finland

* Corresponding author. Legs + Walking Lab, Shirley Ryan AbilityLab (Formerly, The Rehabilitation Institute of Chicago), 355 E Erie St, 60611, Chicago, IL, USA.
** Corresponding author. School of Psychology, University of Nottingham, University Park Campus, East Dr, Nottingham NG7 2RD, UK.
E-mail addresses: julio.hpavon@northwestern.edu, julio.hpavon@gmail.com (J.C. Hernandez-Pavon), Domenica.Veniero@nottingham.ac.uk (D. Veniero).
[1] These authors have equally contributed to this work.

https://doi.org/10.1016/j.brs.2023.02.009

ARTICLE INFO

Article history:
Received 20 July 2022
Received in revised form
10 February 2023
Accepted 19 February 2023
Available online 23 February 2023

Keywords:
Transcranial magnetic stimulation
Electroencephalography
Recommendations
TMS–EEG preparation
TMS–EEG data analysis pipelines
TMS–EEG
TEPs
Artifacts

ABSTRACT

Transcranial magnetic stimulation (TMS) evokes neuronal activity in the targeted cortex and connected brain regions. The evoked brain response can be measured with electroencephalography (EEG). TMS combined with simultaneous EEG (TMS–EEG) is widely used for studying cortical reactivity and connectivity at high spatiotemporal resolution. Methodologically, the combination of TMS with EEG is challenging, and there are many open questions in the field. Different TMS–EEG equipment and approaches for data collection and analysis are used. The lack of standardization may affect reproducibility and limit the comparability of results produced in different research laboratories. In addition, there is controversy about the extent to which auditory and somatosensory inputs contribute to transcranially evoked EEG. This review provides a guide for researchers who wish to use TMS–EEG to study the reactivity of the human cortex. A worldwide panel of experts working on TMS–EEG covered all aspects that should be considered in TMS–EEG experiments, providing methodological recommendations (when possible) for effective TMS–EEG recordings and analysis. The panel identified and discussed the challenges of the technique, particularly regarding recording procedures, artifact correction, analysis, and interpretation of the transcranial evoked potentials (TEPs). Therefore, this work offers an extensive overview of TMS–EEG methodology and thus may promote standardization of experimental and computational procedures across groups.

1. Introduction

Transcranial magnetic stimulation (TMS) has proven to be an effective, non-invasive tool for probing the human brain [1]. The first effort to combine TMS with electroencephalography (TMS–EEG) was reported in 1989 by Cracco and colleagues [2] and later by Amassian and colleagues [3]. However, the technique was not yet ready for broader use as the recorded cortical response was obscured by the TMS-induced electromagnetic artifact. A few years had to pass before the electromagnetic artifact problem was partially solved. In 1996, the first successful TMS–EEG study (published by Ilmoniemi et al. [4]) demonstrated the feasibility of the combination to record cortical excitability and connectivity. After these first successful recordings, the interest in using EEG to measure brain activation elicited by TMS has steadily increased. Consequently, this has opened new possibilities in basic and clinical research as noted in a recent review [5].

More than two decades after the first successful TMS–EEG combination [4], multiple approaches to recording and analyzing the TMS–EEG data have been developed, and there is still no consensus on how to standardize the procedures for TMS–EEG preparation, data acquisition, and analysis. This article aims to review the state of the art in the field and provide, when possible, recommendations for successful TMS–EEG studies to eventually improve the reproducibility of experimental and analysis procedures across laboratories. We aim to share our expertise with the community, based on published data and personal experience. We have gathered several leading TMS–EEG experts, hoping to promote clarification of concepts, improvement of our practices, guidance for newcomers, and identification and addressing of open questions in the field.

1.1. Electrophysiological aspects of TMS–EEG

1.1.1. TMS

TMS excites axons in the brain via inductive electromagnetic stimulation. A strong, very brief, magnetic field is delivered to the brain via a transducing coil. The changing magnetic field induces a time-varying electric field (E-field) in the cortex. Depending on the orientation of the E-field with respect to the geometry of the cortex and cortical neurons, the E-field leads to a depolarization of axons in the stimulated brain area. Depending on the level of depolarization, action potentials may be triggered [6,7] which travel orthodromically (towards the axon terminal) and antidromically (towards the cell body) along the axons [8]. Transsynaptic activation of neurons on which the excited axons impinge will induce postsynaptic currents in the dendritic arbor of cortical pyramidal neurons at the target site. Postsynaptic potentials are subject to summation spatially and/or temporally. If the summation is large enough and involves a sufficiently large area of the cortex, the postsynaptic currents will result in a measurable EEG signal. At the same time, the spread of activation along pyramidal neurons causes a secondary excitation or inhibition of connected subcortical structures and cortical brain regions. The temporospatial summation of postsynaptic currents in the dendritic arbor of pyramidal or other cells in connected cortical areas may also cause a measurable EEG signal, contributing to the transcranially evoked EEG response.

TMS is based on electromagnetic induction, described by Faraday's law. A TMS pulse is initiated by flowing an intense current (~5 kA) through the TMS coil windings. This current produces a time-varying magnetic field that penetrates the scalp and skull unimpeded, inducing an E-field. The brain is a conductor; therefore, eddy currents (i.e., currents that circulate in closed loops and in opposite directions than the currents in the TMS coil) are induced in the brain that can depolarize neurons, producing neuronal firing. TMS is thought to activate cortical neurons that have axonal bends or other geometrical inhomogeneities or endings in the induced E-field, as the E-field along neurites changes most rapidly at these locations [9,10]. The strength of the magnetic pulse is in the order of 1–3 T, with a rise time of about 50–100 μs. Because of the short pulse duration, the temporal resolution of TMS is sub-milliseconds, which allows for real-time modulation of the brain. The spatial extent of the cortical area stimulated by TMS depends on the coil geometry, stimulus intensity, target area, and, therefore, coil-to-cortex distance [11–13]. As magnetic fields attenuate rapidly with distance and as the induced E-field approaches zero at the center of the head, TMS stimulates superficial cortical layers more strongly than deeper layers. However, the induced neuronal activity depends also on other aspects (like the position and orientation of neuronal structures and membrane characteristics). In summary, besides stimulating the target area and surrounding tissues, TMS indirectly activates synaptically interconnected sites, a feature exploited in brain connectivity studies [4]. When the stimulation

intensity (SI) is adequate, locally evoked action potentials may propagate along anatomical connections across cortical layers within the same cortical column and to other cortical and subcortical regions (e.g., Ref. [14]), and may result in the activation of an entire network [15]. The cascade of events that accompanies TMS [12] is described in Fig. 1.

The brain activity evoked by TMS can be recorded with different neuroimaging techniques such as EEG, functional magnetic resonance imaging (fMRI), near-infrared spectroscopy and positron emission tomography (for a review see Refs. [17–19]). However, the most successful and thus commonly used combination has been with EEG because it is a widespread method, is less expensive than other neuroimaging techniques, and is technically the least complicated to be combined online with TMS.

1.1.2. EEG

Despite developments in measurement technology, the basic principles of EEG remain unchanged from Berger's time [20]. EEG, with its millisecond temporal resolution and a spatial resolution of centimeters, is widely used for non-invasively studying the electrophysiological dynamics of the brain [21,22]. EEG measures electrical potential differences between pairs of electrodes placed on the scalp. The recorded signal is a linear mixture of source-current amplitudes, and the signals in neighboring electrodes commonly correlate [23]. The EEG signal is primarily due to the synchrony of postsynaptic potentials rather than action potentials [24]. Action potentials have a short duration compared to postsynaptic potentials; for this reason, action potentials do not overlap as much in time and synchronize much less than postsynaptic potentials. Furthermore, due to their symmetric current distribution, the E-field generated by action potentials decays faster with distance than that of postsynaptic currents [16,22,23,25,26]. Postsynaptic potentials are primarily confined to the dendrites and cell bodies. When a sufficient number of neurons – several thousand or more – with similar overall orientation produce synchronous postsynaptic currents, the resulting E-field and volume currents summate, making it possible to record the cortical EEG response at the scalp level.

1.1.3. TMS–EEG

The combination of TMS with EEG has been relevant for addressing fundamental neuroscientific questions in new ways. In particular, the two techniques complement each other, in that causal information provided by TMS overcomes the correlational nature of EEG data, whereas the ability to record from the whole scalp provides a global picture of the brain activity generated by the E-field. One of the main advantages of using TMS–EEG is that outcome measures, derived from EEG responses to TMS (i.e., evoked potentials or brain oscillations) can be used as a neurophysiological marker of excitability or connectivity for any brain area, including the regions where TMS does not generate a proxy of cortical/cortico-spinal excitability, such as motor evoked potentials (MEPs) or phosphenes [4,27]. Although TMS–EEG data can be analyzed in the time and frequency domains, so far, most studies have focused on the former, the so-called TMS-evoked potentials (TEPs).

1.1.4. TEPs and TMS-triggered oscillations

TEPs are brain potentials time-locked to the TMS pulse [27,28]. To study TEPs, the signal is averaged across trials. The initial TMS-evoked response is presumably produced by the activation of neurons concentrated in the targeted area followed by the activation of axonally interconnected areas [4,29]. Different methods on how to measure the TEPs have been reviewed elsewhere [5,30].

The TEPs consist of positive (P) and negative (N) deflections that reflect a spatio-temporal superposition of excitatory and inhibitory postsynaptic potentials, like the so-called event-related potentials (ERPs) [31]. Although the neurophysiological underpinnings of TEPs remain to be completely elucidated, they are considered a genuine, reproducible measure of cortical reactivity [32–34]. TMS of the primary motor cortex (M1) evokes several peaks, described at approximately 15 (N15), 30 (P30), 45 (N45), 60 (P60), 100 (N100),

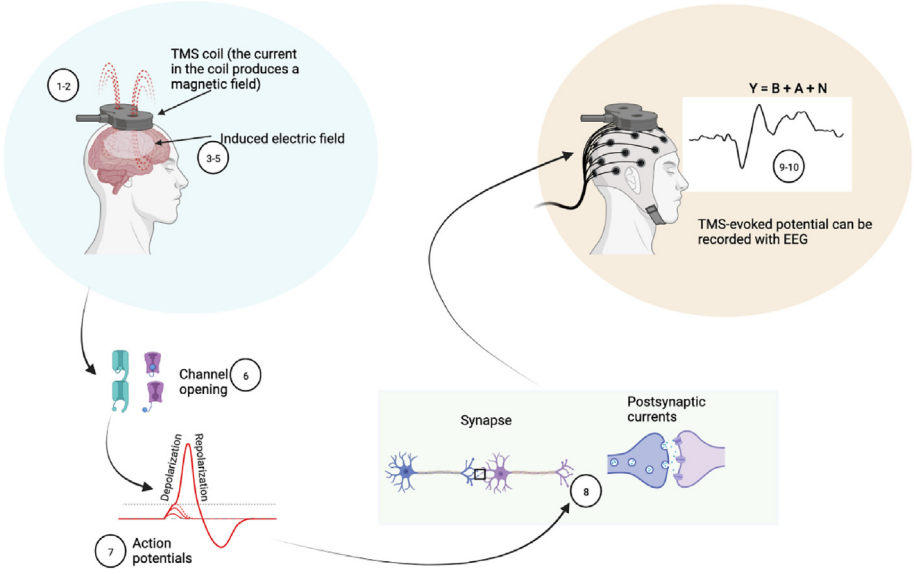

Fig. 1. Chain of events triggered by the TMS pulse. (1–2) A current pulse flows through the TMS coil (max I ~ 5 kA) and produces a brief (~100 μs) but strong magnetic field (max B ~ 1–3 T). (3) The changing magnetic field induces an E-field (~50–100 V/m) in the brain which in turn (4) produces a flow of electric current in the tissue (~0.1 mA/mm^2) (5) The flow of current (i.e., ions). produces local membrane depolarization (>~10 mV). (6) Voltage-gated ion channels are opened and (7) action potentials are generated in axons where depolarization reaches the firing threshold. (8) Neurotransmitters are released in the synaptic cleft. (9) Postsynaptic currents are generated, which lead to postsynaptic excitatory (and inhibitory) potentials that in turn lead to action potential generation if the firing threshold is exceeded. This transsynaptic activation represents the activation of networks. The potential differences (E-fields), resulting from postsynaptic currents, drive volume currents inside the head and the scalp [16]. (10) The TMS-induced activation can be recorded with EEG. Note that the EEG signal can be described with a linear model, $Y = B + A + N$ (see Section 6.1). Figure created with BioRender.com.

and 180 (P180) milliseconds [28,32,35,36]. However, recently it has been shown that later peaks (>~80 ms) such as N100 and P180 may be contaminated by sensory-evoked responses (see **Sections 3.5**, **4.2.3**, and **4.2.4**), while very early peaks, such as the N15, can be contaminated by cranial muscle responses (see **Section 4.2.2**).

TEPs are detectable up to 400–500 ms around the stimulation area as well as in distant inter-connected brain areas [4,32,37]. Accordingly, for some TEP components, the maximal amplitude is recorded by the electrodes close to the stimulation site, while others may be more prominent over distant electrodes, e.g., over the contralateral hemisphere [38]. There is evidence that TEPs are associated to varying degrees with different neurotransmitters (e.g., Ref. [39]). TEP peaks and time courses depend on the stimulated area, coil orientation [37], and functional state of the underlying cortex; the latter may be dependent on factors such as behavior [40], level of consciousness (e.g., Refs. [41,42]), and neuropsychiatric diseases (e.g., Ref. [43]). In addition, TEP amplitudes are influenced by the applied TMS pulse strength (e.g., Refs. [44,45]).

TMS effects on brain activity can be further investigated in the frequency domain. When a cortical area is perturbed by TMS, the neuronal response as measured by EEG tends to oscillate at a specific natural frequency [46–48]. Part of this response may be explained by the phase alignment of ongoing local brain oscillations through the effect of the TMS pulse on the targeted cortex [49]. Therefore, TMS–EEG can be used to manipulate and investigate brain rhythms by measuring the impact of a TMS pulse on EEG and associated behavioral effects [50]. The same methods used to study EEG oscillations can be used in TMS-triggered oscillations [51–53]. Since this topic is out of the scope of this paper and has been widely discussed elsewhere, we refer the reader to previous literature (e.g., Refs. [5,53]). However, researchers should carefully distinguish between TMS-evoked responses (i.e., signals that are phase-locked and thus survive averaging of single trials) and TMS-induced responses (i.e., signals that are not phase-locked and thus cancel out during averaging; e.g., Ref. [54]). The latter requires the calculation of time-frequency representations (TFR) at the single-trial level with subsequent averaging to preserve the oscillatory activity that is related to but not phase-locked to the TMS pulse. Notably, this measure, which can also involve certain baseline normalization operations and is sometimes referred to as TMS-related spectral perturbation (TRSP), reveals a mixture of phase-locked and non-phase-locked responses that are difficult to disentangle [52].

Throughout this paper, we will mostly refer to TEPs when describing EEG responses to TMS, but the same considerations apply to TMS evoked and TMS-induced oscillatory activity, except where otherwise stated.

2. TMS–EEG instrumentation

This section aims to provide a comprehensive overview of the equipment currently available to acquire TMS–EEG data and to discuss how different settings/parameters affect the quality of the recordings. To do so, we reviewed published evidence, reported practices, and experiences documented by different laboratories.

The instrumentation to acquire TMS–EEG data typically includes a) TMS device and coils, b) TMS-compatible EEG amplifier, and c) TMS-compatible electrodes. The integration of a neuronavigation system is highly recommended to keep the TMS coil on the desired target with the same orientation and angulation throughout the session and across visits in the case of longitudinal measurements [32,33,55]. In addition, the use of a neuronavigation system is mandatory in studies involving patients with structural brain lesions, since stimulation of severely damaged areas does not elicit any EEG response [56]. In the following sections, we describe each component.

2.1. TMS stimulators

Currently, there are several TMS stimulators available on the market. When performing TMS–EEG studies, the following properties can be useful.

1. Option to control the recharge delay: a change in the potential of the coil during the capacitor recharging can cause electrical artifacts in the EEG recording. Since the recharging typically occurs in a time window overlapping with the relevant signal, it is crucial to set the time of recharge outside the temporal window of interest (i.e., the recharge delay should not overlap with the relevant post-TMS signal). To meet this requirement, most of the stimulators currently available on the market (for instance, some versions of MagVenture, Nexstim, Magstim, and Deymed stimulators) include a recharge delay option that allows one to choose the recharge time (see **Section 4** for more details on this artifact).
2. Generation of different pulse waveforms: the most used are monophasic and biphasic waveforms, although available stimulators can generate other waveforms, such as half-sine and trapezoidal.
3. Some stimulators can change the induced current direction in the coil: this may be relevant to studying the effect of the induced E-field direction on brain activity.
4. Compatibility with different TMS coil sizes/shapes. For example, this can be helpful to perform multi-site TMS–EEG studies where 2 or more coils are placed on the head.
5. Cooling system to run long protocols: to improve the signal-to-noise ratio (SNR) of TMS–EEG data, it is generally recommended to average a sufficient number of trials. During stimulation, the TMS coil heats up at a rate that depends on stimulation intensity (SI) and may need to stop working upon reaching a specific temperature because of safety issues. Liquid- or air-cooled coils reduce coil heating.
6. Triggering signal communication between TMS stimulator, EEG, and neuronavigation: the communication between hardware is crucial, i.e., controlling properties of the stimulator (like SI, inter stimulus interval/randomization) via an external device or, e.g., a navigation system.

2.2. TMS coils

Currently, there are many different types of TMS coils [57]. Overall, the coil choice depends on the TMS protocol to be performed. Their shape, size, and winding determine the induced E-field and, therefore, the focality and depth of penetration, which impact the brain volume stimulated [58] and, consequently, the TMS-related EEG responses. The most common TMS coil is the figure-of-eight coil [4,59], but so far, there is no systematic study of the effect of the TMS coils on TMS-related EEG responses. In addition, the type of coil may also determine to what extent cranial muscles near the area of interest will be stimulated, affecting the EEG recordings. Therefore, one should be aware of scalp, facial, and neck muscle activations; for instance, the double-cone coil may trigger strong muscle twitches affecting the EEG recordings, e.g., Ref. [60]. Of note, a novel brain stimulation approach has recently been introduced, the multi-locus TMS (mTMS) [61–63], allowing electronically controlled stimulation of multiple brain areas at different times and intensities, (for an example of TMS–EEG and mTMS see Ref. [64]).

2.3. Effect of TMS pulse waveform

In this section, we will briefly outline our current knowledge about the two most common pulse shapes, in TMS–EEG recordings, i.e., monophasic and biphasic waveforms [65,66].

Monophasic and biphasic pulses are defined by the amplitude ratio of the first and second phases of the E-field waveform. Monophasic pulses are shorter (usually around 100 μs) and consist of a steep initial current flow in the coil, which is responsible for neuronal depolarization. A switch or a diode in the stimulator prevents the coil current from flowing in the reverse direction (Fig. 2). Nevertheless, when the coil current (and the consequent magnetic field) returns to zero, an induced current in the brain in the opposite direction is always present. However, this current in the opposite direction only ends the depolarization phase, it will not trigger any action potentials; therefore, the biologically relevant current is monodirectional [67–69].

Biphasic pulses are longer (up to several hundreds of μs) and usually consist of at least two half-cycles of opposite polarity but similar amplitude (thus, with an amplitude ratio close to 1), and a shape that is slightly variable across stimulators. In contrast to monophasic pulses, each coil current phase can effectively stimulate the cortex [67,69], although the second phase contributes to most TMS effects due to its larger change of amplitude and duration [71]. In other words, for a monophasic pulse, the first phase is more relevant for exciting cortical neurons, whereas, for a biphasic pulse, the second phase is more effective. Because of this difference, the monophasic pulse is preferred when investigating the effects of current direction, which are less pronounced with the biphasic pulse [67].

Pulse direction: On a practical note, the pulse waveform and the stimulator brand determine the direction of the current induced in the brain [72]. For example, the optimal current direction of monophasic pulses in the brain tissue for M1 stimulation is posterior to anterior and lateral to medial [73]. To produce this current (by a current changing in the opposite direction in the coil) with Magstim devices, the handle of the coil should point backward for monophasic pulses and forward for biphasic pulses [74]. For MagVenture (MagPro), the optimal current for M1 stimulation with default settings is generated with the handle pointing forward for monophasic pulses and backward for biphasic pulses. The difference between Magstim and MagVenture stimulators is determined by the current direction in the coil, which goes from the handle towards the end of the coil for MagVenture and vice-versa for Magstim (see Fig. 3).

Monophasic and biphasic pulses present unique advantages and disadvantages; the choice will therefore depend on the research question. Previous studies [65] have shown that biphasic waveforms are more effective, i.e., require lower magnetic fields to stimulate the cortex (e.g., lower resting motor threshold) and, therefore, may be preferred for TMS–EEG experiments, given that the severity of many TMS-related artifacts increases with the SI (e.g., muscle artifacts) [75]. Lower intensities will also minimize participants' discomfort.

Different waveforms have been reported to affect the amplitude of the initial TMS artifact but not its duration [76,77]. Following the stimulation of a dummy head, two independent studies reported

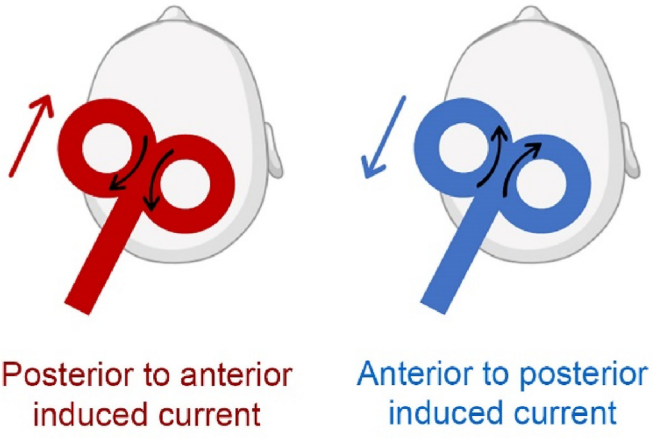

Fig. 3. Example of induced current direction by two different stimulators. In Magstim stimulators (left figure) the current in the coil flows from the top to the handle as indicated by the curved arrows. The current induced in the brain flows in the opposite direction and is therefore defined as posterior to anterior as depicted by the straight arrow. In other stimulators, such as MagVenture (right figure), the opposite is true. The current in the coil flows from the handle to the top as shown by the curved arrows and therefore the induced current in the brain flows from the front to the back, i.e., it is an anterior to-posterior current.

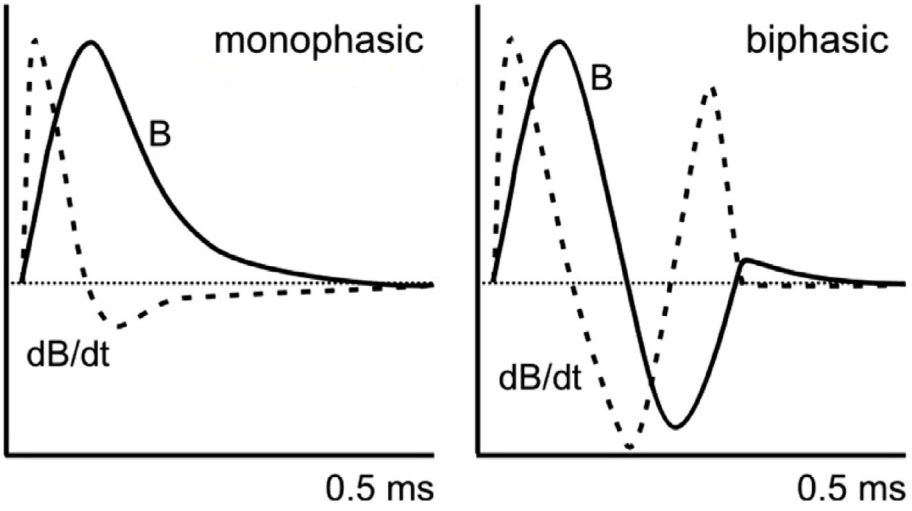

Fig. 2. Comparison of monophasic and biphasic pulses. The monophasic pulse (left panel) consists of a steep initial current flow, whereas the biphasic pulse (right panel) consists of two half-cycles of opposite polarity (see text for a detailed description). The figure shows the time course of monophasic and biphasic magnetic pulse with magnetic field strength B (solid line) and its rate of change dB/dt (dashed line), which correlates with induced electric field strength. Reproduced with permission from Funke [70].

that monophasic pulses induced a larger artifact compared to biphasic pulses, but the EEG signal returned to the baseline levels within 5 ms after the pulse delivery regardless of the waveform type. It is worth noting that, while these results indicate that the artifact duration does not depend on the waveform, the 5 ms interval hinges on the EEG equipment and recording parameters (**Section 2.4**). Furthermore, while the duration of the initial artifact was found to be similar, this does not rule out effects on later artifacts (some of the authors of this paper have indeed reported that the monophasic waveform causes an offset that slows the return of the EEG signal to the baseline).

The effect of the TMS pulse waveform on brain activity has been recently investigated by Casula and colleagues [78] using TEPs. The authors found that TEPs between 50 and 200 ms were characterized by a larger amplitude when evoked by monophasic compared to biphasic pulses [78]. However, the effect of pulse shape on the TEPs has not been systematically investigated and more studies are needed.

2.4. EEG amplifiers

The first methodological challenge associated with recording EEG during TMS is the strong E-field generated by the magnetic pulse, which can saturate the recording amplifiers for several seconds. To overcome this problem, a sample-and-hold circuit was introduced to control the recording apparatus and lock the EEG signal [79]. The circuit held the EEG acquisition for a few milliseconds following TMS delivery [79–81], thereby avoiding saturation of the recording amplifiers and allowing one to record the response generated by the stimulation after the hold period. In more recent years, a different generation of amplifiers has gained popularity and has replaced the sample-and-hold circuit approach. These amplifiers have been designed to work in high time-varying magnetic fields, thus avoiding saturation, and have in principle the advantage of allowing the EEG to be acquired continuously. However, the stimulus artifact covers a small amount of signal, possibly including the initial response of the directly stimulated cortical target, that cannot be recovered with current preprocessing methods (see **Section 4**). For an overview of different TMS-compatible EEG systems, see Supplementary Materials (Table S1 and questionnaires).

Despite the lack of systematic investigations, we know that some recording parameters are more effective than others in limiting the impact of the initial electrical artifact, which is a high-amplitude and high-frequency signal. As shown in Fig. 8 in Freche et al. [82] (see also [83]), and as recommended by many manufacturers (Table S1 Supplementary Materials), an adequate sampling rate must be selected, together with a corresponding low-pass cutoff. The lower the low-pass is, the longer the ripples created by the interaction of the filter with the TMS pulse artifact last. If sampled at very high rates, the pulse artifact lasts only as long as the actual TMS pulse and also reflects the pulse shape. With lower sampling rates (and thus lower anti-aliasing low-pass filters), filter ripples increase in amplitude and duration, and longer pulse artifacts arise. For example, with the same amplifiers and experimental setting, Veniero et al. [77] reported an artifact duration of 5 ms with a sampling rate of 5 kHz, whereas Bonato et al. [37] reported a 10 ms artifact with a sampling rate of 1 kHz.

As reported in Table S1 (Supplementary Materials), all TMS-compatible EEG amplifiers can record data with a high sampling rate. It is worth mentioning that some companies report that with a sampling rate of ~20 kHz, the artifact duration is below 2 ms or even below 1 ms when sampling at 80 kHz (in line with Freche et al., [82]). However, the definite end of the pulse-ripple artifact can be difficult to determine objectively (but see [77]).

To avoid further rippling, additional low-pass filters must be avoided where possible or carefully chosen. While low-pass filters reduce the pulse artifact amplitude, they increase its duration. Since the EEG signal covered by the pulse artifact cannot be recovered and is later removed, its amplitude and clipping can be ignored, and one should aim to reduce its duration as much as possible. For similar reasons, DC amplifiers are to be preferred over AC amplifiers, since high-pass filters also interact with the pulse artifact and introduce artificial trends/drift in the signal around the TMS pulse (for a detailed discussion on high-pass filters effects, see [84]). Of note, high-pass filters can also tamper with later artifacts and TEPs. For DC amplifiers, either no high-pass filters or a very low one (e.g., 0.016 Hz, i.e., 10 s time constant) should be used to prevent/reduce such trends.

For a list of available TMS-compatible EEG systems see Supplementary Materials, where we report the results from a questionnaire, we have asked several manufacturers to fill out with general information about each system.

2.5. EEG electrodes

In standard EEG, four types of electrodes can be used: passive, active, dry, and sponge. However, conventional EEG electrodes cannot be used with TMS [28,85] because the magnetic pulse induces eddy currents (i.e., currents that circulate in closed loops) and causes electrode heating. These issues can be reduced using sintered Ag/AgCl pellet or C-ring electrodes (i.e., ring electrodes with a slit to prevent current induction in a closed ring), which have been used in most TMS–EEG studies. A disadvantage of pellet electrodes is the considerable amount of preparation time required to reduce the impedances to acceptable values (5 kΩ or less). The so-called *Multitrodes* (EasyCap) are C-ring electrodes in which the Ag/AgCl coating is located on the inner instead of the lower surface of the C-ring. Since the contact surface is larger and more easily accessible, many authors of this paper have reported that impedances can be lowered more quickly. C-electrodes are usually preferred because they reduce eddy currents induced by TMS, which may contribute to the decay artifacts (see **Section 4.1.3**).

2.5.1. Active vs. passive electrodes

Active electrodes (AEs) have been introduced in electrophysiology only in recent years. Compared to traditional passive electrodes (PEs), which act as simple recording sites, AEs entail preamplification of the signal directly at the electrode stage. When recording standard EEG, this feature provides several advantages, such as the reduction of electrical line noise and the recording of a better signal at higher electrode impedance levels. In addition, the ease of montage and the fast preparation of AE recordings result in shorter experimental sessions and a reduction of discomfort for participants.

Recently, a few studies have used AE with new active amplifiers to record EEG during TMS [38,86–88]. One of these studies directly compared the performance of AE and PE by looking at TEPs [86] and revealed no significant difference in amplitude or scalp topography. However, some AE users have observed an increase in the decay artifact (see **Section 4.1.3**) duration that should be further investigated. Moreover, while AEs reduce the preparation time, their larger thickness increases the coil-to-cortex distance and requires higher TMS intensity, which might impair the EEG signal quality and lower the spatial specificity of the stimulation. This also unfavorably affects the activation threshold and should be acknowledged when reporting and comparing threshold values between studies [89]. Overall, while AEs seem a useful addition to the TMS–EEG field, more studies are needed to assess their performance in different experimental settings.

2.5.2. How many electrodes do we need to record acceptable EEG responses?

A common question in the field is how many electrodes should be used. The original International 10–20 system was devised with the intention that each electrode would inform about brain activity in the underlying cerebral structure [90]. The electrode potentials were usually measured with respect to the same reference electrode, resulting in controversial discussions about the proper reference electrode location. Currently, as we understand the sensitivity patterns of the EEG signals, we do not need to worry about the reference electrode "problem". Referencing is a linear data transformation therefore the data can be re-referenced offline. Unless the reference position is particularly prone to local artifacts (from movement, sweating, TMS, etc.), a later re-referencing to the common average (or any other preferred linear recombination) allows recovering the reference signal, so that the referencing during recording is arbitrary.

Each electrode derivation measures the difference between two scalp potentials, informing us about one dimension of the source current distribution in the brain. This dimension, described by the sensitivity pattern or lead field of the derivation, depends on the placement of the electrodes as well as the details of the conductivity distribution of the head. When the number of electrodes is increased after the first few dozen, the marginal benefit of each new recording channel diminishes quickly because nearby electrodes sense nearly the same potential [91]. It has been found that the rank of the data obtained with a large electrode set is typically 30–50, meaning that with optimal placement on the scalp, 30–50 electrodes would be enough to gather the spatial information that is available to EEG [92–94]. Because the electrode placement is usually not optimized, about 60 electrodes (in practice often 64) is sufficient to obtain almost all signal components available from scalp recordings [92].

However, a couple of advantages *are offered by a larger number* of electrodes. First, if an electrode channel becomes noisy or non-functional in a 256-channel system, virtually no spatial dimension is lost, since the redundant channels can provide the lost information. Second, if one can assume that the noise in neighboring electrode channels is statistically independent (as it is if the noise is mainly from the electrode contact and the amplifiers), the overall SNR is increased; in effect, signals from neighboring channels will be effectively averaged in the course of data analysis. Thus, because the source-level SNR is in principle approximately proportional to the square root of the number of channels with uncorrelated noise, increasing the number of electrodes from 64 to 256 could double the source-level SNR [95]. In fact, some data-cleaning methods, such as the source-estimate-utilizing noise-discarding algorithm (SOUND) algorithm (see **Section 6.3.3** for details), utilize cross-validation between channels to detect the channel-specific noise. For these methods, "oversampling" the EEG spatially is beneficial when estimating the noise distribution. However, SNR improvements can be obtained also by improving electrode contacts and by lowering the noise level in amplifiers. Third, artifacts due to the activation of cranial muscles could be more accurately pinpointed with additional electrodes. Since TMS activates muscles only under the coil, in some experiments it would suffice to add just a few muscle-activity-detecting electrodes over the TMS target area. The extra electrodes would enable one to measure and model the spatial pattern of the electrical activity of the muscle so that the artifact could be removed from the rest of the data.

2.6. Neuronavigation

Neuronavigation has become increasingly important in TMS research, as it increases stimulation accuracy and efficacy [96,97]. With navigated TMS (nTMS), the coil position and orientation can be monitored in real-time, ensuring appropriate stimulation of the target area throughout the experimental session [28,98,99]. This reduces possible inter-trial variability in the TMS–EEG recordings due to coil movement and increases accuracy by reducing the risk of stimulating a slightly different area [100]. As neuronavigation systems can store information on the coil position and orientation, they also ensure comparable targeting across multiple sessions and result reproducibility [55,101,102]. Some systems can mark EEG trials when displacements from the target occur.

Advanced neuronavigation systems compute the induced E-field in the brain, which enables precise anatomical stimulus targeting; the strength of the E-field serves also as a stimulation intensity that is independent of coil or stimulator type (see **Section 3.2**). Using nTMS to align the direction of induced current relative to the underlying gyral pattern is furthermore expected to increase TMS effectiveness. The strength of stimulation is enhanced when the current is perpendicular to the target gyrus relative to when it is parallel (for modeling see Ref. [103]; for an application including parallel currents as control, see Ref. [104]) (see also **Section 3.4**). Existing nTMS systems estimate the induced E-field using spherical conductor models to take into account the local curvature of the skull [105] and display the results on the individual anatomical MRI to assist with the coil positioning [98,99]. Another approach to improve targeting and accuracy consists of using realistically shaped boundary element head models [106,107]. While TMS–EEG studies may benefit from using neuronavigation systems based on realistic head models, such models have not yet been implemented online due to the computational cost [106].

Robotized nTMS has also been used in combination with EEG to assess the effect of coil position accuracy on TEPs [108] and to map EEG responses of several brain areas [109]. The idea is that automatic positioning allows us to target many cortical areas in a reasonable amount of time with high precision. A caveat of robot-navigated TMS–EEG, however, can be increased levels of line noise in the EEG data from the electronics of the robot, which may require a spacer-mediated gap between the TMS coil and EEG cap and/or additional grounding measures.

3. General aspects of TMS–EEG

3.1. Number of trials (Signal-to-noise ratio)

One of the most common questions people in the EEG and TMS–EEG community ask is "How many trials do I need to acquire in my experiments to obtain meaningful TEPs or oscillations?". Although these are simple questions, they do not have a simple answer.

The number of trials depends on the meaningful signal in relation to the noise content, i.e., the SNR. The SNR depends on the square root of the number of trials [110], provided that the meaningful signal and noise remain similar from trial to trial. In more detail, let S be the size of the signal, N the size of the noise on a single trial, and T the number of trials. The SNR on a single trial is defined as S/N (the signal divided by the noise). The total SNR of averaged responses, such as TEPs, is then equal to $(S/N) * \mathrm{sqrt}(T)$ (the single-trial SNR multiplied by the square root of the number of trials). The closer the meaningful signal level gets to the level of noise, the more trials are required. However, if the meaningful signal is below the noise level in a single trial, even more trials are required. The required number of trials also depends on the set quality criterion, i.e., the required SNR. Suppose the required SNR is known and the single-trial signal level and noise levels are known. In that case, the required number of trials can be calculated. As noted above, the increase in SNR is not linear; therefore, doubling

the number of trials does not double the SNR. For instance, to double the SNR from 100 trials, one needs to measure 400 trials. This means that, after a certain point, increasing the SNR further would lead to very lengthy experiments without significant benefit. The power law of SNR has additional positive implications. When a sufficient number of trials have been recorded, one should not be too concerned to reject contaminated epochs, as this will have only a minor impact on the potential maximal SNR. For instance, after recording 300 trials, one can reject 30 trials and decrease the theoretical maximal SNR by only 5%.

When TEPs are the signals of interest, a good starting point to set the number of trials could be looking at studies that have investigated test-retest reliability and reproducibility [32,33,86,87,111,112]. Many of these studies suggest that around 100 *clean trials* (note: clean refers to the number of trials after exclusion of artifactual epochs) are sufficient to have reliable TEPs. However, most studies have been performed on motor areas and therefore, this conclusion might not apply to other areas. Additionally, weak cortical responses tend to require more trials than strong cortical responses. For example, it has been reported that the reliability of the TEP peaks is dependent on the investigated component, and the concordance between trials plateaus after 60 trials, while the smallest detectable difference continues to improve with added trials [33].

Since the amplitude of the cortical responses is related to the applied SI, low intensities tend to require more trials [45]. Rosanova et al. [113] suggested that the number of trials needed for a high SNR range between 150 and 300, depending on the intensity of stimulation (as an empirical rule, the higher the intensity, the lower the number of trials). While this is a good approach, care should be taken since the strength of the cortical response varies from one location to another [32,33,55,114], and increasing the SI may also have an impact on TMS-induced activation of cranial muscle, voltage decay, and sensory evoked potentials. Therefore, different target regions might require a different number of stimuli. For instance, stimulation of frontal areas is more prone to artifacts than motor areas and a larger number of trials may be required since there is a higher likelihood of rejecting bad trials due to artifacts (e.g., eye-blinks and muscle contractions). However, following good practice during TMS–EEG preparation and recordings might help to decrease noise and get better SNR (see **Section 5**) with a reasonable number of trials.

The number of trials should also be chosen considering the type of outcome measure we are interested in. Therefore, we recommend referring to the relevant EEG literature to define the number of trials. As an example, indexes related to the frequency domain, such as pre-stimulus phase estimation are known to depend strongly on the number of trials (for a review see [115]). TMS–EEG data do not constitute an exception, as demonstrated by Schaworonkow et al. [116], who confirmed that if the measure of interest is the phase of the EEG signal immediately preceding the TMS pulse, the phase-estimation algorithm depends strongly on SNR.

3.2. TMS threshold determination

There are several ways to determine the TMS SI or threshold, which depend on the outcome measure of choice and a somewhat arbitrarily defined criterion. Thresholds can be determined by measuring motor responses, phosphene perception, in principle also the amplitude of TEPs, or estimated by simulations of the induced E-field.

Motor responses: The most common way to determine the SI is to measure the motor threshold (MT) in a resting muscle. This is done by first mapping the M1 cortical representation for the target muscle and then finding the optimal position and coil orientation, for that muscle, thereby maximizing the E-field at the cortical representation area ("hotspot") of the muscle. The MT is measured by directing the E-field to the hotspot and is typically defined as the minimum TMS intensity able to evoke MEPs of at least 50 μV peak-to-peak in the contralateral muscle of interest (to the stimulated hemisphere) in 5 out of 10 consecutive trials e.g., [117,118]. Of note, due to TMS-induced E-field spreading and overlapping cortical representations, MEPs are also elicited in muscles adjacent to the one examined [119]. The interstimulus interval (ISI) between consecutive TMS-pulses should be set sufficiently long to avoid cumulative effects (e.g., Refs. [120,121]); evidence exists that ISIs of 5 s or longer increase the reliability of MEP measurements [122,123]. It is also beneficial to jitter the ISI to avoid any expectation and habituation effects [123,124]. If the SI for TMS–EEG measurements is based on the MT, one should consider using the same ISI and jitter for threshold estimation and TMS–EEG protocols.

Although the MT is measured from M1, it is commonly used to set the SI in non-motor areas as it is simple, fast (depending on the exact MT determination method), it can be reliably determined with a number of pulses as low as 17 [125], and provides a highly replicable measurement [126,127]. The limitation of this approach lies in the assumption that sensitivity to TMS for non-motor areas is similar or correlated to that of M1. This does not seem to be the case, for example, see Stewart et al. [128] for a comparison between phosphene and MT (but see [129]). In addition, TMS–EEG studies support different responsiveness to stimulation for different cortical areas [32,35,55]. Unique cytoarchitectonic features could affect how a brain region reacts to TMS. Also, simple anatomical features such as variations in scalp-to-cortex and, therefore, coil-to-cortex distance have to be taken into account; this is automatically done in navigation systems where the cortical E-field is computed (see below). In TMS, the magnetic field decreases with the square-distance; therefore, the farther the coil-to-cortex distance, the weaker the magnetic field and the induced E-field in the cortex. As the coil-to-cortex distance varies between brain areas/targets, it is challenging to know which percentage of MT should be used for other areas, and practices on how to adjust the TMS intensity vary substantially between research laboratories (for a simple metric to account for coil-cortex distance see [130]).

Instead of recording motor responses with the EMG, some groups determine the TMS threshold by visually observing muscle twitches. However, this approach overestimates the MT and is not considered suitable for reproducible measurements [131] and standardizing methods across users. Visual observation of muscle twitches can be useful to ensure that the recorded MEPs mainly reflect the target muscle of interest.

Phosphene perception: In visual areas, the SI can be based on the phosphene threshold (PT). Phosphenes are illusory percepts, often described as visual flashes perceived immediately after the TMS-pulse, thought to occur from the direct activation of the visual cortex [132–134] or fiber tracts such as the optic radiation projecting into the visual cortex [135]. The PT is calculated similarly to MT, but rather than relying on objectively measurable responses (i.e., MEPs), it depends on the participants' subjective report (they are asked to indicate the presence/absence of phosphenes). As the relevant parts of the visual cortex may be located deeper than the primary motor cortex, the PT is typically higher than the MT [128,129,136]. An additional limitation is that phosphenes can only be elicited in around 60% of participants [137,138] and, therefore, MT is sometimes used to set the TMS intensity if no consistent phosphenes can be obtained [104,137].

Induced E-field: Another way to determine the SI is to calculate the induced E-field at the target and select the TMS intensity that generates the desired E-field [98,99,139,140]. Inherently, and

ideally, this method is not dependent on the coil-to-cortex distance [141] and can be used for any cortical area. One limitation is that this technique requires the use of advanced neuronavigation and participants' MRIs (see **Section 2.6**), which might not always be available. Furthermore, the online E-field calculation is only available in a few TMS/Navigation systems (for which the underlying algorithms for E-field estimation are not openly available). However, open-source software, which takes into account the subject-specific anatomy, for offline E-field modeling is available (e.g., www.simnibs.org [107]); and is now widely used in the field of transcranial electrical and magnetic stimulation. In contrast to accurate finite-element calculators, such as Simnibs, commercial online E-field estimators are based on computational simplifications. For instance, one such neuronavigation system is based on computing the E-field inside a sphere, fitted to the local subject-specific geometry. The computational differences between different systems can lead to discrepancies in the E-field estimations across different studies. Thus, online E-field monitoring might be most useful to normalize the TMS dose within a cohort and to ensure test-retest reliability within a subject.

Finally, the relationship between the TMS-induced E-field and the activation of the target site has to be further investigated. Factors influencing neuronal excitability such as axonal geometry may affect the required E-field in a way that is difficult to predict based on a priori information, i.e., we do not know the intensity and orientation of the E-field that should be applied to effectively stimulate the cortex. Previous studies have shown that when stimulating the visual cortex: a) with E-field intensities below 50 V/m, post-stimulation activity is indistinguishable from baseline EEG activity (i.e., no TEPs could be elicited); b) TEP amplitudes progressively increase with the intensity of the induced E-field; c) at 120 V/m there is a substantial activation of the target area [142] with the same intensity, there is a clear differentiation in the TEP frequency content across stimulation sites [46]. Importantly, E-field estimates do not consider the possible effects of other factors such as the TMS pulse waveform and duration or the spatial extent of the E-field with a certain intensity, which may contribute to the temporal and spatial summation of the induced activations and thus to the ability of a TMS pulse to evoke action potentials in cortical neurons.

TEP amplitude: The SI can also be determined by searching stimulus parameters that maximize TEP amplitudes. In analogy with the motor hotspot search, the position, orientation, and intensity of the TMS can be adjusted to optimize the impact of the stimulation on the underlying neuronal circuits while minimizing artifacts at the same time. This approach relies on the visual inspection of the data in real-time during the recording (rt-TEP software, [34]). At first, visualization of single-trial data allows to immediately assess the presence of evoked muscle activity or other TMS-related artifacts; if the cortical target is not too close to cranial muscles, small adjustments of coil orientation and/or position are often enough to reduce the impact of these artifacts on the EEG signal [75]. Subsequently, the effectiveness of the stimulation can be evaluated by measuring peak-to-peak amplitude of average TEPs (re-referenced to the average reference) obtained after a limited number of pulses (e.g., 20-trial average) in the first 50 ms after TMS in the channels closest to the stimulation site. Specifically, EEG responses to TMS are expected to show larger amplitude a) in the channels close to the stimulation site compared to distant channels, b) at early latencies compared to late latencies, and c) in the channels of the stimulated hemisphere compared to the contralateral ones. Based on these TEP features, the peak-to-peak amplitude of the largest component measured in the first 50 ms in the channel closest to the stimulation site represents a readout of the impact of TMS on the cortex. The reliability can be further enhanced by combining multiple EEG channels into linear combinations that enhance the sensitivity of the readout to the region of interest.

The peak-to-peak amplitude of the early and local EEG response to TMS after averaging 20 trials correlates with the signal-to-noise ratio of a full session in which 80–100 trials are averaged and depend on the amplitude and variability of spontaneous EEG (see Supplementary results in Ref. [34]). Although it is not possible to set an absolute value for the ideal peak-to-peak amplitude, in principle it could be possible to estimate a reasonable endpoint based on the number of trials to be collected and on the amplitude of ongoing EEG activity.

This approach implies that the effects of TMS parameters (intensity, site, orientation) are assessed in real-time and adjusted (if needed) to minimize muscle artifacts and maximize the strength of the initial cortical activation; thus, it may imply a deviation from precise targeting requirements (e.g., while stimulating over cortical sites associated with a certain assumed function or dysfunction), for improving data quality. In conclusion, relying on a real-time EEG readout during the experiment provides immediate control over undesired artifacts. This approach is most effective while stimulating cortical structures close to the midline where cranial muscle activation can be reduced by small adjustment of TMS parameters and becomes more challenging when more lateral cortical areas are targeted [75].

3.3. Required/optimal TMS intensity to induce brain activity

The SI will have an impact on whether only local TEP components are evoked or a wider network is activated, for instance by transcallosal pathways [143–147]. Several studies have described the input-output characteristics of TMS–EEG responses, i.e., how they change as a function of the SI, and they mostly indicate a linear relationship at typical SIs, at least on M1 and prefrontal cortex (e.g. Refs. [45,148], but see Ref. [138] for non-linear intensity–amplitude relationship in visual areas). In other cases, SI may be defined through known behavioral effects from the literature, hence ensuring suprathreshold SI. For instance, in a recent series of TMS–EEG experiments on Frontal Eye Fields (FEF)-control over posterior brain signals, Veniero et al. [50] used a fixed SI of 65% of maximum stimulator output (MSO), which was defined based on prior studies revealing that exactly this intensity effectively activates FEF and its projections as inferred from behavioral TMS effects on visual attention tasks [149–151] and perception tasks [152]. In the study by Veniero et al. [50], FEF-TMS at this suprathreshold SI (relative to behavioral effects) led to changes in intrinsic brain oscillations at occipital sites, i.e., in remote connected areas. Besides suprathreshold SI, there is also evidence that subthreshold SI (with respect to MT) can be sufficient to induce TMS–EEG responses, albeit likely confined to the local level. It has been shown that stimulation of the left and right M1 and prefrontal cortices at 60% MT is sufficient to evoke measurable brain activity [35,148], and E-fields of around 40 V/m in the targeted neuronal tissue may be sufficient to produce neuronal excitation [144,147]. In M1, this E-field strength can induce visible TMS–EEG peaks, but these SIs (commonly less than 50% of MT) may not be enough to activate the whole motor network [144]. There is also some evidence that the excitation threshold may depend on neuron types and local neuronal circuits (e.g., Ref. [13]).

The question about the SI necessary to activate transcallosal and other long-range pathways, as detected with TMS–EEG, is still open and will also depend on the population under investigation (e.g., brain responses of patients with major depression are altered when compared to healthy volunteers (e.g., Ref. [153]).

3.4. The effect of coil location and orientation

It is well-known that coil location and orientation affect the MEPs [73,154]. These parameters also influence TEPs [32,37,55]. However, in TEPs these effects have not been studied as extensively as in MEPs, as the impact of only a few coil orientations and locations has been tested. Different coil orientations influence TEP polarities [78] and amplitudes [55], although not all components are equally affected [37,78,108]. In some participants, varying the coil location near the hotspot slightly influences TEP amplitudes, whereas, in others, it also affects the TEP waveform [108]. Coil orientation also influences brain oscillations, as reported in a study by Thut et al. [104], where the magnitude of the entrained alpha oscillations was at its maximum when the coil was oriented to induce currents perpendicular to the target gyrus [103].

3.5. How to deal with the EEG responses caused by co-stimulation of peripheral structures of the nervous system

TMS typically causes somatosensory and auditory sensations because it might not only activate cortical neurons, but also nerves innervating the face, jaw, and neck muscles. Even when no muscles are activated, the pulse causes scalp sensations due to the excitation of afferent nerves (e.g., trigeminal nerve) or to mechanical stimulation of the skin by coil vibrations (e.g., a tapping sensation). In addition, a clicking sound is produced by the coil wires when the pulse is discharged and can activate auditory pathways through air and bone conduction. These sensory inputs may lead to peripherally evoked EEG responses which contaminate transcranially evoked EEG responses that result from direct cortical activation. The peripherally evoked potentials may not only contaminate transcranially evoked EEG responses but may also modulate them through neurophysiological interactions.

Recently, a few articles have triggered an intense discussion in the TMS–EEG community, opening a debate about the extent to which EEG responses to TMS are caused by direct cortical stimulation or include potentials elicited by sensory input associated with TMS [155–157]. Therefore, more attention has been paid to the use of control and sham stimulation during TMS–EEG experimentation. In the following, we will discuss strategies that can be used to control for peripherally evoked EEG responses, the most suitable depending on the experimental design and aim of the study [158].

Several procedures have been proposed to deal with the auditory stimulation that accompanies the TMS pulse delivery. Some strategies assume the linear summation of the activity generated by TMS and the auditory activation. Here, TEPs are recorded without the presence of masking noise, and the auditory evoked potential is mathematically removed either with the use of independent component analysis (ICA)-based approaches or by recording an additional auditory sham session that will be subtracted from, or at least compared to, the contaminated TEPs. Another strategy consists of controlling for auditory stimulation by playing a continuous noise to mask the coil click, such as white noise, colored noise, or a noise adapted to the spectral characteristics of the click itself and tailored in real-time based on participants' perception [41]. Recently, Russo and colleagues [159] developed and shared a tool to easily implement the latter solution with any type of coil and stimulator and to manipulate the standard noises in both time and frequency domains. Crucially, the use of this tool and the generated customized noise has been demonstrated to be effective at lower volume intensities (quantified by sound pressure level measurements) compared to the standard noises. It should be noted though that noise-masking may introduce a change in functional resting-state brain connectivity similar to the effect induced by scanner noise during fMRI [160]. This change in “brain state” might alter the brain's responsiveness to TMS.

While there is reasonable evidence that air-conducted auditory evoked responses can be suppressed by masking noise, at least under certain experimental conditions [38,41,56,161], the TMS click may still elicit auditory responses through bone conduction [162,163]. Furthermore, as suggested in some cognitive studies, somatosensory evoked potentials (SEP) might be modulated by the white noise [164]. Studies are warranted to systematically assess whether or how concurrent noise exposure shapes the TEPs. Instead of masking the coil click with additional noise, one may try to reduce the coil click as much as possible. Recently, a TMS coil with substantially reduced acoustic noise has been developed by attaching the windings to a surrounding damping casing separated by an air gap [165]. The acoustic noise of the coil click was reduced by 18–41 dB. However, this coil has not been tested in TMS–EEG experiments yet.

Complementing the efforts to mask or minimize auditory and somatosensory co-stimulation, several groups have used “realistic sham stimulation” to replicate the coil click and the sensation of a real magnetic stimulation without significantly stimulating the brain tissue [166]. However, establishing an effective sham stimulation procedure is a longstanding issue in the TMS literature and remains problematic [167]. In TMS–EEG experiments, one option that has been explored is complementing TMS with cutaneous electrical stimulation. The TMS coil is used to reproduce the clicking noise, whereas electrodes attached to the scalp [38,156,167] or to the coil itself [60] are used to apply electric stimuli intended to mimic the somatosensory input associated with real TMS [168]. Despite all efforts to develop a realistic multisensory sham stimulation, none of the reported procedures have been able to perfectly match the peripheral co-stimulation of real TMS (see, for instance, Refs. [38,167]). This is mainly because the somatosensory percept related to TMS and electrical stimulation are qualitatively different and can be distinguished by the subjects [38,156,167].

A different way of dealing with spurious activations is to implement a comparative strategy as is typically done in fMRI experiments [169], that permits isolation of the effect of interest. If the study aims to evaluate the effects of an experimental manipulation (e.g., learning), a pre/post-test design offers the advantage of testing the same participant at different timepoints, i.e., before and after the intervention, with the same TMS parameters. Likewise, studies that aim at testing the task-dependent modulations of TEPs may include recordings with the same TMS parameters in different task conditions. If this is the case, the sensory stimulation will be the same across time points or conditions, and differences in EEG can be attributed to direct cortical stimulation, provided that the experimental manipulation does not change the processing of sensory input. This strategy has been used in several TMS–EEG studies (e.g., Refs. [170–174]). The “comparative strategy” assumes that the interventional protocol does not change the peripherally evoked EEG response elicited by TMS. Although this might not always be the case it should be controlled when needed for the research question and protocol. Participants might habituate or become sensitized to peripheral co-stimulation, introducing order effects on peripherally evoked EEG responses in TMS–EEG experiments. The intervention itself may directly modulate the peripherally evoked EEG responses or indirectly by changing the arousing or attentional effects of peripheral co-stimulation on the TEP.

A similar comparative strategy has been applied in studies aiming at characterizing excitability and connectivity of a brain area in different states or during a task. In this case, the experimental design should include conditions that can be compared to answer the research question. Not many studies have used TMS–EEG

during a cognitive task, but in this case, having a control task while keeping the stimulation parameter constant would ensure equal sensory stimulation. As an example, Morishima et al. [175] traced FEF connectivity in a face discrimination task and compared it to the same measure obtained in a motion discrimination task (note that faces and moving dots were presented simultaneously). Another approach entails the use of TMS pulses delivered at different intervals from an event of interest (e.g., movement onset, visual stimulus). The comparison of TEPs evoked during different "tasks", "task epochs", or "states" can still be influenced by task-specific, epoch-specific or state-specific modulations of the central processing caused by peripheral co-stimulation (e.g., resulting in gating or attentional shifts).

In TMS studies without EEG, a control site is often used to control for unspecific effects and establish site-specificity. However, the stimulation of different sites may induce distinct scalp sensations and muscle activation [75,176]. Others have explored the possibility of applying TMS controls over the same site but changing coil orientation from a more effective orientation (E-field induced perpendicular to the target gyrus) to a less effective orientation (E-field parallel to the gyrus) [104]. This should keep peripheral activation similar across conditions (e.g., from sounds), although differences in somatosensation due to different muscle fibers being activated by the two coil orientations cannot be excluded.

Therefore, many approaches have been explored but no consensus has been reached yet on the best approach. It is important to consider EEG responses caused by co-stimulation of peripheral structures when designing a study and apply the solution that is most reasonable for the purpose of the study.

3.6. Triggering of TMS based on EEG features "open- and closed-loop"

Resting TMS–EEG can provide valuable information about the general excitability state or connectivity of the cortex. However, the information obtained about the causal role of specific brain phenomena, such as cortical oscillations, is limited, because there is no obvious way to control these activities. Triggering TMS based on the current brain state can directly probe the role of different cortical functions. There has been some confusion regarding the terminology when it comes to brain-state-dependent *vs*. -independent and closed- *vs*. open-loop TMS (for a recent discussion see Ref. [177]). Triggering TMS in real-time, based on particular EEG features (e.g., oscillatory phase and amplitude of specific frequency bands), allows brain-state-dependent TMS as compared to brain state-independent TMS. The latter is when TMS is applied through some predefined sequence (e.g., with a certain ISI ± some jitter) and therefore disregarding the current brain state. Beyond brain-state-dependent stimulation, closed-loop operation requires that a particular parameter of a system is monitored continuously and that TMS parameters (control signals) are adjusted (e.g., intensity and timing of TMS) accordingly to achieve, maintain, or change the monitored parameter as desired (e.g., aiming at a particular kind of brain state). The prime example of a closed-loop is a thermostat that measures the temperature and modifies the flow of hot water to a radiator to reach and maintain a preset temperature value. However, if the control signal does not change the monitored parameter (e.g., if TMS does not change the monitored brain state), and if this change does not feed back to the stimulation parameters, the loop remains open [178]. All studies published so far, therefore, represent at best open-loop brain state-dependent TMS–EEG since TMS-related EEG artifacts and peripheral co-stimulation evoked/induced responses currently still prevent continuous EEG monitoring in real-time.

An open-loop real-time approach is represented by the TMS pulse to the brain delivered at a predefined brain state (e.g., phase), implying that the induced brain response (e.g., TEPs) does not influence the characteristics of the next TMS pulse. In essence, the state of the brain is used to guide the TMS, delivered based on a parameter decided a priori, allowing an improvement in testing the brain response in specific conditions. The other approach is defining a closed-loop, which implies controlling the brain state via TMS to reach and maintain the TMS-induced response within a predefined range. In this condition, the induced brain response provides feedback for adjusting the TMS parameters via a feedback loop [179].

In this context, EEG–TMS (i.e., TMS guided by EEG) can be used to characterize the physiology of endogenous oscillations, both in terms of phase-dependent excitability (e.g., which phase of the sensorimotor μ-rhythm corresponds to maximum corticospinal excitability) [180–183] but also phase-dependent plasticity [181,184]. The promise of such EEG-triggered TMS protocols is not only that a stronger and more reliable plastic response may be achieved at the site of stimulation, but also that specific neural pathways may be modulated, when synchronizing the stimulation with EEG-derived brain connectivity states.

In terms of signal processing, whereas the pre-stimulus EEG period is unaffected by the TMS artifact, averaging cannot be used in the same way to remove random noise. Since each trial must be considered individually, signal quality issues (baseline fluctuations, eye blinks, periods of low amplitude in the oscillation of interest, etc.) are critical. Especially slow drifts caused by the previous TMS pulse when recording in DC mode can be problematic; this needs to be considered in the preparation and online signal processing pipeline.

When using oscillatory brain activity as a "state marker" to trigger TMS, the state effects will critically depend on the method used to capture the ongoing oscillatory activity [183]. Due to the limited spatial resolution of EEG, the oscillatory activity at the sensor level may reflect a mixture of activity from various cortical regions rather than being generated locally in the cortex targeted by TMS [185].

4. The artifact problem in TMS–EEG: non-physiological and physiological signals

The TMS pulse can induce different artifacts, which can be of non-physiological or physiological nature. These artifacts can be time-locked or non-time-locked to the TMS-pulse. Both have been described in several publications [27,28,85,186–188]. In this section, we review known EEG artifacts generated by TMS, clarify their nature and present possible solutions to deal with them.

4.1. Non-physiological artifacts

Non-physiological artifacts are induced by the TMS pulse, and their origin is electromagnetic or mechanical.

4.1.1. Pulse artifact or electromagnetic artifact

This is the largest artifact generated by the TMS pulse (Fig. 4). It is electromagnetic in nature and is produced by the electromotive force induced in the loops formed by EEG electrode leads. It can be up to several volts, masking the brain signals and saturating EEG amplifiers, limiting the use of simultaneous TMS–EEG.

Solution: this artifact cannot be avoided; however, TMS-compatible EEG amplifiers have been developed, allowing one to handle this artifact (see Supplementary Materials for a list of TMS–compatible EEG systems). The best strategy we have is to reduce the pulse artifact duration to its minimum. As explained

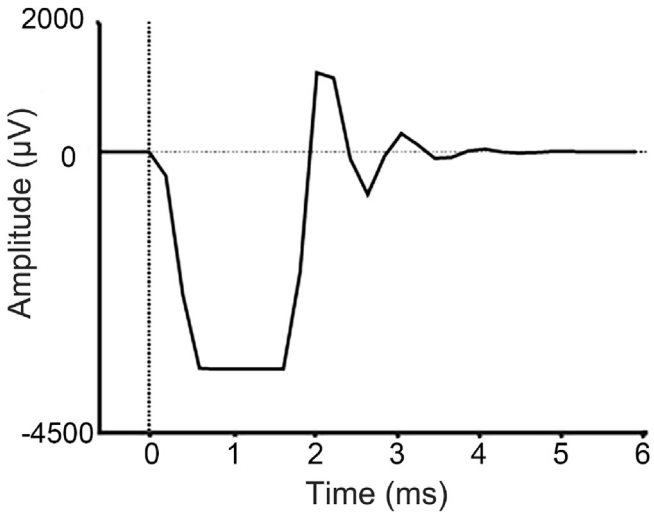

Fig. 4. TMS pulse artifact recorded using a sampling rate of 5 kHz and an anti-aliasing low-pass filter of 1 kHz (resulting in filter ripples or 'ringing'). In addition, signal saturation can be observed for the first large negative deflection around 1 ms.

before, a sufficient dynamic range, adequate sampling frequency, and high-enough cut-off frequency for the anti-aliasing low-pass filters can reduce the artifact duration significantly.

4.1.2. TMS recharge artifacts

This artifact is produced when the capacitors, which store the electric charge required for TMS, are recharged. The recharge artifact can look like a spike, an abrupt signal jump, an exponential decay, or a waning high-frequency discharge, depending on the TMS device used (Fig. 5). This artifact can corrupt the EEG recordings and be mistakenly interpreted as a brain signal, particularly if low-pass filtering is applied or TFRs are calculated before inspecting the data.

Solution: in newer TMS stimulators, the timing of the capacitor recharge can be manually adjusted; therefore, the recharge artifact can be delayed and set to occur outside of the time window of interest. When the stimulator does not allow us to adjust the delay, it is important to determine the exact onset of the recharging from the manufacturer or by performing phantom recordings [77] to facilitate the offline removal and interpolation of uncorrupted signals. It is important to note that, in some TMS systems, the recharge delay may vary depending on the SI, although there would be a consistent latency at a given SI [77].

Additionally, in some devices, brief (few ms) low amplitude spikes may be visible, which are not time-locked to the TMS pulse but reflect maintenance recharging of the capacitors while idling (this can be observed in some MagVenture stimulators). Custom modifications of the device allow to transiently prevent maintenance recharging for time windows of interest. Alternatively, moving median filters (width of a few ms) allows for post-hoc removal.

4.1.3. Decay artifact

Different authors have referred to this artifact as decay artifact, discharge artifact, or electrode polarization artifact [28,34,186,187,189]. In many cases, the electrode–skin interface can be polarized by electric currents between the electrolyte gel and the recording electrode. When an electrode is polarized, it might take hundreds of milliseconds after the TMS pulse for the charges to return to equilibrium. This typically leads to an exponentially decaying

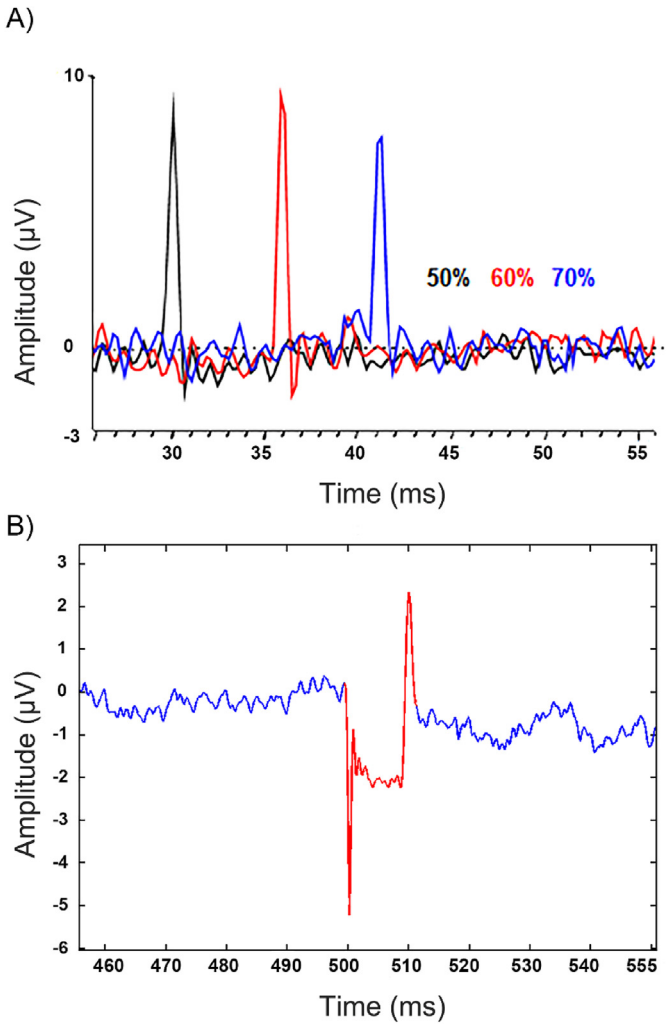

Fig. 5. Example of recharge artifact. A) When the recharge delay is not set by the experimenter, the Magstim Standard Rapid^2 generates a recharge artifact that peaks at different latencies depending on the stimulation intensity. In this example, the artifact peaked at 30, 36, and 42 ms after the pulse delivery at an intensity of 50, 60, and 70% of MSO respectively. Note that the amplitude of the artifact does not change with the intensity. B) Recharge artifact caused by the MagVenture MagPro X100 when the recharge delay is set at 500 ms from the pulse delivery (Modified from https://www.fieldtriptoolbox.org/assets/img/tutorial/tms-eeg/art_recharge_2.png).

charge, the decaying current being proportional to the remaining polarization voltage [82]. Note that the artifact can consist of several different decaying components with different time constants.

Solution: polarization artifacts can be minimized by choosing non-polarizable electrode materials and electrolyte, as well as by low contact impedance. By ensuring the best possible conductance between the scalp and the electrode, one can shorten the time constant of the capacitive behavior of the electrode–skin connection, thus shortening the lifetime of the artifact. Low impedances (that can be further minimized by mini-punctures of the skin) have been shown to reduce the size of the pulse and decay artifacts [190]. Decreasing the impedance of the skin dramatically reduces skin potentials [191]; this is relevant because skin potentials are slow shifts that can lead to an increase in low frequencies that affect the EEG recordings. Finally, minimizing the impedance of the skin–electrode interface decreases the thermal voltage noise [192,193].

4.1.4. Electrode motion artifacts

This artifact is very common [194] and is of mechanical origin. It is caused by the movement of the electrode against the electrolyte gel and of the latter against the skin. This artifact may occur for several reasons: a) it may result from the vibration of the TMS coil transmitted to the electrodes via direct contact, as well as repelling magnetic force caused by the electric current induced in electrode and wires by the magnetic pulse [79,195]; b) muscle twitch/head movements induced by the TMS pulse; c) the coil or operator touches the electrodes; d) movement-related skin stretching causing skin potential shifts [196]. The motion artifacts that are induced by the pulse delivery either directly (a) or indirectly (b) usually occur within the first ~10 ms after the TMS pulse and are usually masked by the pulse artifact, the cranial muscle response, and the decay artifact. As an exception, artifacts generated by skin-stretching resulting from cranial muscle contractions can last longer [196]. However, as recently reported [197], artifacts can simply result from the contact between TMS coil and EEG electrodes and affect both pre- and post-pulse EEG activity.

Solution: the electrode motion artifact and in general, contact artifacts, can be reduced by placing a thin layer of foam between the coil and electrodes and wrapping the EEG cap with a cellophane layer (this is done in some labs, although one should make sure that no additional artifacts are induced by sweating) and/or an elastic net bandage. 3D printable spacers for separating the TMS coil from the electrodes to prevent electrode movement have been designed and tested [197].

4.2. Physiological artifacts (TMS-locked)

Eye blinks, cranial muscle twitch, auditory responses to the coil click, and SEPs, are all physiological but unwanted signals that can be induced by the TMS pulse. These responses are true physiological signals that can confound the true TEPs, i.e., the neuronal response to the transcranial stimulation of the brain tissue, and complicate their interpretation (see **Section 3.5**).

4.2.1. Eye blinks and eye movements artifacts

Eye blink artifacts occur spontaneously and are very common in traditional EEG recordings. They result from a strong dipole consisting of positive and negative poles at the front and back of the eye, respectively. The dipole maintains a strong and stationary electrical field potential, which extends to the surrounding parts of the head, the field falling off gradually toward the back of the head [198,199]. Eye movements slightly modulate the dipole, causing a substantial deflection in the EEG. Ocular artifacts can be induced by TMS as part of a startle reflex due to the coil click.

Solution: training of the subject can help decrease TMS-elicited startle-related eye-blink artifacts. Spontaneous eye movements (not triggered by TMS) are less severe than the TMS-induced ocular artifacts as the former are not time-locked to the TMS pulse and therefore statistically independent of TMS-evoked activity and thus easier to remove from the data using techniques such as ICA. To prevent spontaneous eye movements (not triggered by TMS) during recordings, a fixation cross could be provided for the subject (if no behavioral task is used).

4.2.2. Cranial muscle artifact

These artifacts can be induced by the TMS pulse when muscles innervating the head/face are stimulated and can strongly contaminate the EEG. They are thus time-locked responses and not to be confused with the typical muscle artifacts observable in EEG-only recordings, originating from tonic muscle activity or spontaneous movements. The TMS-evoked muscle artifacts are often biphasic deflections and up to 3 orders of magnitude stronger (~mV) than the neuronal responses (μV) with a variable duration that depends on the activated muscle (~10–30 ms possibly followed by a slow return to baseline, Fig. 6). Muscle artifacts peak within milliseconds after the pulse delivery, thus heavily affecting the early responses to TMS [75,200]. These artifacts may result either from depolarization of intramuscular motor nerve endings or from activation of cranial motor nerves, such as the facial trigeminal nerves [201]. Therefore, they represent compound muscle action potentials (just like those in hand muscles when applying TMS to the median nerve). Most likely to be activated are neck, facial [202], frontal, temporal, or masseter muscles, depending on the placement of the TMS coil [75,76]. Consequently, large artifacts are likely to be elicited depending on the proximity of the TMS target to lateral aspects of the head [75], language areas such as Broca's and Wernicke's areas (by activation of temporal muscles, e.g., masseter muscle) [200,203], and dorsolateral prefrontal cortex (by activation of frontal and orbicularis oculi muscles) [36]. Note that cranial muscle contractions can lead to electrode movements and stretch the overlying skin, which leads to related disturbances in the electrode–electrolyte–skin interfaces and electrode motion artifacts, respectively. Consequently, the topography of decay and muscle artifacts is often coupled, with particularly large/long decays for electrodes overlying cranial muscles.

Solution: one practical solution to reduce muscle artifacts is to move the location or change the orientation of the TMS coil. However, this may not be always possible if the target coordinates or research questions are strictly constrained. Reduction of the TMS intensity or use of smaller, more focal coils can also be beneficial to decrease muscle artifacts (Section 3). However, when the muscle artifacts cannot be avoided during TMS–EEG data acquisition, certain artifact removal methods can be used offline to remove or suppress the muscle artifacts (see Section 6.3).

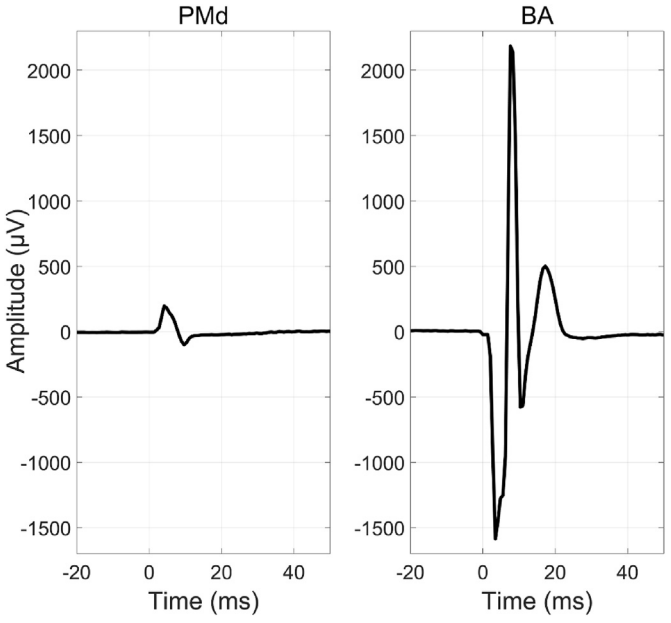

Fig. 6. Muscle artifacts. Waveforms after stimulating the dorsal premotor cortex (PMd), and Broca's area (BA) in a representative subject. Those signals correspond to the responses recorded with electrodes near the respective stimulation sites. The artifacts in both PMd and BA are much larger than the brain signal. The amplitude of the artifact in BA is about 3500 μV peak-to-peak. The artifacts that arise after stimulating lateral brain areas mask the brain signals because they can be several orders of magnitude larger than the brain signals and last for tens of milliseconds.

4.2.3. Auditory artifacts

The magnetic field generated by the TMS coil produces strong forces on the currents in the coil windings, which results in a loud click. This sound has been shown to produce an auditory evoked potential. These responses are maximally expressed at the vertex, in a time window approximately from 100 to 200 ms, and can confound TMS-evoked brain activity analysis [38,156,163,167,204]. Also, general arousal due to TMS or auditory inter-sensory facilitation by the coil click might be present.

Solution: auditory responses can be dampened by combining noise masking with hearing protection so that the coil click becomes attenuated or imperceptible [38,41,173]. Part of the sound is still transmitted to the inner ear through bone conduction [162,163], but this can be attenuated using a piece of foam between the coil and the scalp [142] (but see Ref. [205] for less convincing effects of foam padding). The effectiveness of the auditory dampening/masking procedure should be validated empirically for each study. Different setups have been previously used: a) Masking composed of white noise mixed with specific time-varying frequencies of the TMS click (e.g., Ref. [49]), with a specific procedure now available as an open-source toolbox [159]. b) Earphones playing continuous white noise, where the white noise is always kept below 90 dB [142,206]. c) Earplugs plus ear defenders. d) Earphones playing continuous white noise plus ear defenders on top of the earplugs [38,205]. Another approach to control for auditory confounds is to introduce a realistic sham condition and/or comparative strategies (see Section 3.5). It is worth noting that some of the authors are currently unsure as to whether noise-masking procedures themselves affect TEPs (see for example [164,207]). Finally, new solutions have been developed to produce quieter coils [61,208].

4.2.4. Somatosensory responses

TMS may cause somatosensory peripheral co-stimulation via several mechanisms: a) the coil vibration can activate mechanoreceptors in the skin, b) the pulse may directly activate local peripheral sensory axons, c) entire sensory cranial nerve bundles may be activated (e.g., branches of facial, trigeminal, occipital nerves), d) cranial muscle twitch induced by TMS (see previous sections) can result in afferent volleys from muscle afferent fibers. This peripheral co-stimulation may induce unwanted SEPs and oscillatory responses that are not triggered by the transcranial activation of the cortex. However, SEPs have not been fully characterized in the TMS–EEG literature, due to difficulties in reproducing the somatosensory stimulation induced by TMS independently from cortical activation.

Solution: there is no agreed-upon solution to this unwanted signal because the best strategy will depend on the aim of the study. As previously pointed out, a foam layer between coil and skin can reduce bone-conducted auditory input [163] and might decrease somatosensory activation induced by coil vibration as well. If compatible with the study design, small changes in TMS coil position/orientation may reduce the peripheral co-stimulation of nerve trunks, but in most cases do not remove it completely. Additional strategies can include a so-called realistic sham [156,167,209] and/or active control conditions (e.g., Ref. [175]) that control for somatosensory confounds by experimental design (but see Section 3.5 for a discussion on the limitations of the different approaches).

4.3. Other artifacts

4.3.1. Artifacts unrelated to TMS

In addition to TMS-induced artifacts, other events may disturb the EEG recordings. These include electrical interference from radio broadcasts, mobile phones, computer monitors, line-frequency currents, pumps, air conditioning, elevators, etc. Therefore, nearby electrical equipment can interfere directly with the EEG system, especially if grounding arrangements in the laboratory have not been done correctly, for example if there are ground loops. Physiological artifacts, such as electrocardiographic and respiratory signals, tonic and phasic muscle activity, spontaneous movements (including blinking and swallowing), and sweating, can also contaminate the EEG recordings. EEG can also suffer from skin potentials and thermal noise (see Section 4.1.3).

Solution: some of these artifacts can be removed by using electrically shielded rooms or offline filtering, the latter *only after the TMS artifact has been removed* (Section 6.2). The main recommendation is to keep any devices that cause noise far from the EEG cap and to instruct the subjects to delay any form of voluntary motor activity outside the time windows of interest. Reducing the contact impedance between the skin and the electrode also helps to remove the common mode accurately to suppress the amount of line noise coupled to the EEG leads [210]. In addition, if a laptop is used to record EEG data, some authors recommend unplugging the laptop during the recording. However, this has not been systematically tested and might depend on the EEG system. Also, using notch filtering during data preprocessing can significantly reduce electrical noise, but see Section 6.2 (Temporal filtering) for filters-related issues.

4.3.2. Filtering artifacts

Typically, the filters applied to EEG are designed to attenuate noisy and uninteresting frequencies. For example, low-pass filtering is used to remove high-frequency signals from the data. Filter design is often based on the assumption that the target signal power and phase content are stationary. When the assumption is violated, for example when the signal presents sudden changes, such as steps, peaks, or deflections, artificial oscillatory activity in the data around these phenomena may be caused; this is often termed ringing [211]. One can unintentionally interpret such oscillations as brain-produced EEG activity. In TMS–EEG, filtering over the pulse artifact and the evoked EEG signal can induce ringing around the short-term events. This also applies to any residual artifacts or discontinuities that might be introduced in the signal during data analysis. For example, filtering of the EEG signal after interpolation used to remove the pulse artifact can induce ringing if the timepoint post pulse is not at baseline level (see Section 6.2) because of cranial muscle or decay artifact.

Solution: during data acquisition, any unnecessary low-pass filters should be avoided and the cut-off of the (often implicitly applied) anti-aliasing low-pass filter increased by using appropriate sampling frequencies. During data analysis, both finite-impulse response (FIR) and infinite-impulse response (IIR) filters may induce ringing, but in general, IIR filters are more vulnerable to rapid events than FIR filters, and higher-order filters are more sensitive than those of lower-order. It is noteworthy that any downsampling requires anti-aliasing low-pass filtering. Thus, downsampling should be avoided before the abrupt high-amplitude artifacts are removed from the data.

There are also filtering techniques specifically tailored for discontinuous/non-stationary data. Robust detrending [212] applies polynomial fitting for trend detection after excluding the poorly fitting data (with spikes/steps, etc.). This type of detrending is applicable for TEPs as well. To diminish the amplitude of ripple (rapidly changing noise) signal in single-trial TEPs, Wiener-estimation-based filtering can also be used [213].

It should be critically considered whether filtering is required to answer the research question at hand. If so, before temporal filtering, spatial filtering or other techniques must be used to

remove the TMS-related artifacts. After filtering, it is good practice to visually verify that the filtered and original signals are aligning sensibly, as residual artifacts or signal discontinuities can produce considerable ringing if filtered.

5. TMS–EEG preparation

The best way to deal with artifacts is to avoid them [186]. Therefore, the first step to recording good quality data is to perform high-quality experiments. While many steps for standard EEG preparation can be applied to TMS–EEG (for a comprehensive guide to record EEG data see Ref. [214]), additional steps are required to minimize the impact of confounding factors and artifacts introduced by TMS. In Section 4, we described these artifacts and have already reported some specific requirements for TMS–EEG preparation, e.g., very low impedances (<5 kΩ), positioning of reference and ground electrodes far from the stimulation target, proper selection of the EEG amplifier settings (hardware filtering bandwidth, sampling rate, amplitude resolution). In this section, we present a summary of the procedures carried out across different laboratories and describe several steps that can be considered to improve data. Tips reported in this section are based on a short survey carried out among the authors of the paper (full results can be found in the Supplementary Materials).

5.1. EEG preparation

1) Before placing the EEG cap, cleaning the forehead, the skin around the eyes, and locations where the reference and ground will be placed with an isopropyl alcohol pad will help lower the impedance. For the reference and ground electrodes, some of the authors gently abrade the skin with sandpaper or abrasive gel after (or before) the area has been prepped with an alcohol pad (see question 4 in the survey).
2) As for any EEG study, it is important that the EEG cap tightly fits the participant's head. It may be helpful to measure the size of the head before the recording as described by Farrens et al. [214]. If the 10–20 system is used for reporting electrode locations, the Cz electrode should fall exactly halfway between nasion and inion and halfway between the left and right preauricular points, the central line should be straight and on the midline. Importantly, always check the EEG cap condition (e.g., dirty/broken channels, etc.).
3) The placement of ground and reference varies across laboratories and depends on the stimulation site, the amplifiers, and on whether the available EEG system allows choosing their position (see survey for a brief overview). Placing the reference far from the TMS coil is advisable to reduce interference and to avoid spreading high-amplitude, TMS-locked artifacts to all channels [77]; this seems to be a popular choice (survey question 22). For instance, if the TMS pulse is delivered to the left M1: a) the reference electrode can be placed on the right mastoid and the ground electrode over the right cheekbone; b) the reference electrode to the right mastoid and the ground electrode next to it. c) reference and ground electrodes on the forehead. In any case, ensure that a stable signal can be obtained from the reference electrode. Central midline channels are often used as a reference in EEG research to achieve a tight fit, little movement, no underlying muscles, etc.
4) Additional electrodes can be used to record electrooculogram (EOG), electrocardiogram (ECG), and muscular responses. Electrodes for horizontal and vertical EOGs can be placed as described by Farrens et al. [214]. The required number of electrodes depends on the aim of the study (questions 7, 8).
5) Preparing cap-electrode contacts is a standard procedure in EEG experiments. This can be done using abrasive electrode paste and/or conductive gel (question 9).
6) Electrode impedances are crucial in TMS–EEG studies. There seems to be a consensus on keeping this value ≤ 5 kΩ (survey question 12).
7) Once all the electrodes have been prepared, an additional check is to ensure the EEG system is recording the signal. Standard practice is to ask the subject to blink and tense the jaw muscles to check that the signals are visible. If all electrodes are noisy, the reference and ground could be the problem or external devices might be interfering. In addition, some researchers ask the participant to close their eyes to see if the alpha rhythm is increased over the occipital electrodes to test that EEG works as expected.
8) We can then move to neuronavigation, if available, and perform all the associated procedures, such as fixating the head tracker, and registration of landmarks. *Optional:* For source analysis, electrode digitization/registration is recommended to construct an accurate subject-specific EEG head model.
9) A practice performed in some laboratories is to place a thin piece of foam between the TMS coil and the scalp to reduce somatosensory and bone-conducted auditory evoked responses and electrode motion artifacts. This should be done already when determining the optimal coil placement and MT, to avoid biasing the SI due to the added thickness of the foam ([215]; see survey questions 19, 20).
10) Provide hearing protection to the participant (e.g., earplugs plus ear defenders) and carry out the navigation to find the hotspot (see **Section 4.2.3**).
11) Find the SI (**Section 3.2**). It is worth mentioning that if masking noise is used, it might be appropriate to calculate the SI while playing the noise.

5.2. Online/pseudo-online monitoring of TMS-evoked EEG

Once the EEG and neuronavigation have been prepared, and the TMS target (hotspot) and SI set, a recommendable step before starting TMS–EEG recordings consists of "*online or pseudo-online monitoring for data quality*".

1) Some EEG systems have online interfaces to monitor the quality of the TEPs, in other cases, a simple MATLAB or Python script can be implemented to look at the data offline, or real-time TEPs visualization toolboxes can be used [34,216].
2) At this point, noise-masking can be provided if necessary (see **Section 4.2.3** for alternative solutions to control for the auditory artifact). White noise with ear defenders or earplugs plus ear defenders can be used. Note that the defenders or headphones may interfere with the coil positioning, depending on the area being stimulated.

If white noise is used, this should be adjusted to mask the coil click. This can be done by increasing the volume of the noise until participants can no longer hear the click. If responses are present, then adjust the masking noise parameters and do the step again. Details on this procedure can be found in the recent work of Casarotto et al. [34] and Russo et al. [159]. However, depending on SI and the particulars of the individual subject, some may not be able to tolerate the noise-masking at volumes sufficient to completely mask the TMS pulse stimulus.

3) Changing the electrode wire arrangement to minimize the effective areas of loops formed by electrode wires (and the head) can reduce the TMS-induced artifacts [217]. While optimal cable positions may not be achievable due to the complex shape of the magnetic field and the geometry of the human head, it may be worth optimizing cable locations for the most crucial electrodes (i.e., those at the stimulation site, and reference, and ground; see survey questions 16, 17).
4) An online or offline graphical user interface (GUI) can be used to monitor the quality of the EEG signals [34,216]. For example, one could deliver 10–20 TMS pulses and look at the average responses to check the EEG quality. Then, if needed, cable orientation can be changed as well as small adjustments in coil position and/or orientation, if this does not affect the study protocol. Looking at average responses allows us to evaluate whether the impact of TMS on the cortex is strong enough to elicit a measurable response. For the online approach before looking at average signals, it is necessary to look at single-trial data and possibly reduce muscle artifacts. This procedure has been fully described in Casarotto et al. [34].
5) Once the artifacts have been reduced and the TMS–EEG responses are acceptable, some experiments may benefit from placing a plastic wrap and/or a net bandage around the cap. The plastic wrap prevents the electrodes from drying out during very long recordings, direct electrical contact between TMS coil and gel, and gel smearing by coil movements. Of note, avoid moving or touching the navigation tracker; you can make a hole in the plastic film to go through the tracker. The wrap and the elastic net also keep cables in place (as artifact shape can change when wires are moved, impeding proper post-hoc artifact removal). They also slightly press the electrodes against the scalp and ensure that proper contact is maintained throughout the recording.

6. TMS–EEG data analysis

6.1. Linear model in EEG

The linear model that relates the recorded electrical signals (EEG) to neuronal events can be described by equation (1).

$$\mathbf{Y} = \mathbf{B} + \mathbf{A} + \mathbf{N}, \tag{1}$$

Here, **Y** is the EEG recorded signal, **B** the brain signals of interest, **A** the sum of the artifacts (e.g., TMS-induced artifacts), and **N** is the noise (e.g., background signal) that contaminates the recorded data [213,218]. **Y** is a signal matrix whose entry $Y_{i,t}$ contains the measured value of channel i at time t. The brain responses, **B**, can be represented as a product of two matrices $\mathbf{B} = \mathbf{LS}$, where **L** is the *lead field* or *mixing matrix* whose entry $L_{i,j}$ determines the sensitivity of channel i to the source j, and **S** is the source matrix whose entry $S_{j,t}$ denotes the *amplitude* of the source j at a time t *(the* jth *row* S_j *contains the whole-time courses of source* j*)*. Similarly, the elements $A_{i,t}$ and $N_{i,t}$ of matrices **A** and **N** add artifacts and noise to the recorded signal $Y_{i,t}$.

L is in general restricted to be sensitive to only those sources that are expected a priori to be responsible for the measured signal. Therefore, **L** is made zero in areas where neuronal sources are not assumed to be situated (such as the skull, outside the head, or the white matter). Typically for EEG, the signal is assumed to be produced by postsynaptic currents in the cortex, modeled with a dense grid of discrete current dipoles (typical cortical model consisting of 1000–10000 dipoles) [16,219]. Often, a further assumption is made that, due to their geometrical organization, mainly the pyramidal neuron populations are responsible for the detected EEG signals [23,219]. Thus, **L** is often defined such that it maps only postsynaptic currents that are orthogonal to the cortical surface. The column vectors of **L** hold the EEG topographies of the possible intracranial postsynaptic sources, whereas a row of **L** describes the sensitivity profile of an EEG channel to all the brain sources.

Equation (1) can be further written as

$$\mathbf{Y} = \mathbf{LS} + \mathbf{L}_A\mathbf{S}_A + \mathbf{L}_N\mathbf{S}_N, \tag{2}$$

where $\mathbf{L}_A$, $\mathbf{S}_A$, $\mathbf{L}_N$, and $\mathbf{S}_N$ are the artifact-mixing-, artifact-signal-, noise-mixing-, and noise-signal matrices, respectively. The columns of mixing matrices define the EEG topographies of different artifact and noise components, whereas the rows of signal matrices contain the time courses of the corresponding components. **Section 6.3** describes the different analysis strategies to separate the recording **Y** into the unknown source, artifact, and noise components present in equation (2).

6.2. TMS–EEG pipelines for analysis

Analyzing the data is another major challenge in TMS–EEG experiments because different experimental arrangements (e.g., EEG amplifiers, electrodes, TMS coils and their positions, TMS electronics, etc.) can result in different artifact profiles. Thus, it is not always possible to use the same pipeline for analyzing data collected with different setups. Furthermore, the question of which pipeline is most effective in preserving the neuronal signals of interest while minimizing artifacts is extremely difficult to answer without ground-truth, especially for data containing high-amplitude artifacts like TMS-evoked muscle activity, (for a recent review see Refs. [213,220]). Nevertheless, some steps are similar across laboratories and should always be performed independently of the experimental arrangement. The EEG signals are a linear combination of multiple sources (as discussed in **Section 6.1**) and can be explained with methods of linear algebra. However, the problem again arises due to the TMS pulse which can produce different artifacts complicating this linear relationship. Therefore, TMS–EEG and standard EEG analysis differ mainly because we need to change the order of some of the steps. Furthermore, once a pipeline has been selected, even changing the order of the steps within the same pipeline could change the amplitude and topography of the TEPs [112,220]. For these reasons, as mentioned in **Section 5**, it is crucial to minimize the presence of artifacts during the recording session.

In this Section, we describe commonly used processing steps for TMS–EEG data and outline some considerations for each of these steps. The order in which they should be used is out of the scope of this paper and has been discussed to some extent in previous papers [112,213,220]. *Here we do not provide or recommend any pipeline for TMS–EEG data analysis*. The different offline methods for removing TMS artifacts are discussed in **Section 6.3**.

The benefits of any signal-processing method depend on the validity of the underlying assumptions or knowledge. For example, removing line frequency interference with a narrow band-stop filter will not be successful if the suppressed frequency band is not correct. Also, this is particularly important for TMS–EEG, ICA may incorrectly divide the signal into components if the underlying components are not sufficiently independent. Here, statistical independence means that observation of features of one signal does not provide any information about features of the other signal. If TMS elicits both a brain signal and an artifact signal, these signals are not independent, because the observation of, say, a TMS artifact informs us about the fact that TMS was administered, from which one knows that a brain signal may have been elicited as well. In such a case, the benefits of ICA are not guaranteed.

6.2.1. Epoching data around the TMS pulse

A common early step in processing TMS–EEG data is to epoch the data around the TMS pulse, like other event-related EEG paradigms. The amount of data required before and after the TMS pulse depends on the intended analysis. For time-domain analysis, sufficiently long segments of signals are required before the pulse to allow baseline correction and after the pulse to capture the TEPs, which can last up to 400–500 ms after TMS. For frequency-domain analysis, enough data are required to enable sliding-window time-frequency decomposition, which needs a certain length of data before and after any given time point. For time-domain analysis, epoching the data from −500 to 500 ms around the TMS pulse is reasonable, whereas for the frequency domain the exact length depends on the frequency of interest and analysis parameters (for example, the number of cycles included in the wavelet and frequency of interest).

Another important aspect to consider is "when" epoching is performed. Temporal filtering is often applied after epoching and removal of the pulse artifact to avoid ringing around the pulse. However, applying filters across epoch boundaries (i.e., the start and end of the epoch) can result in additional artifacts due to zero-padding, especially for high-pass filtering. One approach to minimize this issue is to include enough data before and after the pulse so that these boundary artifacts have time to recover and do not impact data of interest (e.g., the baseline period or the TEPs). This could be done by initially having a longer epoch and then redefining the trials after high-pass filtering or by 'mirroring' the epoch (i.e., flip and concatenate the data at either end of the epoch). Alternatively, a solution is to remove the pulse artifact and apply high-pass filtering to continuous recordings before epoching [159]. In any case, no high-pass filtering is to be applied before the TMS pulse and other high amplitude artifacts have been removed from the data.

6.2.2. Removing bad channels/trials

A common strategy for minimizing noise is to remove the affected data from the signal. For example, channels can be removed from the data if they have become disconnected during recording, or if they show persistent artifactual activity due to poor contact, ongoing muscle activity, or contact with the TMS coil. In addition, individual epochs/trials can be removed if they are affected by artifacts such as excessive muscle activity (e.g., due to jaw clenching, swallowing, or activation of facial muscles), large blinks or eye movements, and other movement artifacts (e.g., if the participant moved or scratched their head). Strategies for selecting which channels/trials to remove vary from manual methods in which the experimenter visually assesses the data and decides which channels/trials to remove, to automated methods which use features of the signal and statistical approaches to identify artifactual data for removal, to combined automated/manual approaches.

While removing affected data is a highly effective strategy for reducing noise, it also comes at a cost. For example, if an artifact is present across many channels/trials, then a large amount of data will be removed, leaving little data containing the signal of interest. This can pose a particular problem for TMS–EEG signals which often contain many contaminated channels in the vicinity of the stimulation target, which often also overlay the region of interest on the cortex. Removing (or topographically interpolating) channels also reduces the rank of the signal, which can impact subsequent processing steps such as ICA. Furthermore, removing channels often results in an unbalanced montage across the scalp, which invalidates the assumptions of average re-referencing and therefore requires additional processing steps to interpolate the missing data, see Section 6.2.9. *Interpolate removed channels.* Also, many types of artifacts can effectively be removed using ICA (e.g., eye blinks, muscle noise, etc.), and removing entire trials or channels beforehand may unnecessarily sacrifice those data. On the other hand, ICA may be occupied by single bad electrodes or trials, reducing the ICA's capacity for capturing other, more relevant artifacts. Therefore, sometimes a tedious iterative process of artifact rejection and ICA application may be required.

6.2.3. Removing and interpolating the TMS pulse artifact

The time-varying magnetic field of TMS results in a high-amplitude pulse artifact in EEG recordings. The most common approach to deal with TMS pulse artifacts is to remove and replace the affected data. There is no consensus on the time window to be interpolated, as the pulse artifact duration depends on the EEG system and setup, in particular the sampling rate and related anti-aliasing low-pass filter, but usually, the interpolation starts 1–2 ms before the pulse and lasts up to 5–10 ms after the pulse, either on epoched or continuous data. This step is not required in EEG systems that use sample-and-hold circuits (e.g., the Nexstim eXimia EEG system).

To avoid additional artifacts, it is crucial to replace the removed data with cubic interpolation rather than linear interpolation [187,221]. As the EEG signal in the first milliseconds after the TMS pulse may not be at baseline level when early-latency artifacts are present (e.g., electrode polarization/decay artifacts, TMS-evoked muscle artifacts, etc.), linear interpolation can generate a transient in the data and result in ringing artifacts or spurious power in TFRs following temporal filtering. Replacing the missing data with interpolated data generated using a cubic (instead of a linear) function can help minimize this effect by smoothing the transition between the real and interpolated data.

In any case, the smoothness of the data should be carefully inspected after interpolation to ensure that no residual artifacts, step responses, and signal discontinuities exist. If necessary, interpolation duration needs to be extended or its method changed to obtain better results. If spatial filters or other artifact removal techniques follow, interpolation may be repeated/refined thereafter, when the removal of muscle/decay artifacts may have minimized the vertical offset of the interpolation endpoint in the post-TMS period.

It is noteworthy that the interpolated data segment must not be used as input for ICA or principal component analysis (PCA). As interpolated data is artificially generated, it can also affect these statistical methods in unpredictable ways. It is thus good practice to simply cut out the interpolated data windows before feeding data into a spatial filtering method and use them only for visualization or when required for temporal filtering.

6.2.4. Re-referencing the data (mean reference/average reference)

As for EEG recordings, data are usually recorded against a single reference electrode and are often re-referenced against either the common average of all cephalic electrodes or a non-cephalic reference (such as linked mastoids or earlobes) to allow topographical interpretation of the signals. Note that the common average reference is most widely used, but artifacts from bad channels might thereby spread to all other channels, and these must be removed (or excluded) beforehand; also note that the removal of bad channels may result in an asymmetry of the common average reference. Therefore, interpolation of removed channels may be necessary before common average reference. The use of a common average reference is also useful to compare data across laboratories since the positioning of the physical reference may vary (for a comprehensive discussion about referencing see Ref. [219]).

6.2.5. Baseline correction

Another common step in TMS–EEG analysis is to 'zero' or 'baseline correct' the data by subtracting a given value from all data points, thereby centering the voltage from each electrode around a common reference value. For TMS–EEG data, the baseline correction should be in a time window that does not contain the TMS pulse (for instance, −500 to −10 ms). Baseline correction is necessary because factors such as skin hydration and static charges in the electrodes may cause an offset in the EEG recordings. Furthermore, this step can be quite important as TMS–EEG data are often collected without a high-pass filter (i.e., with amplifiers in direct current or DC mode), meaning that the 'baseline' voltage can differ substantially between electrodes and their signals are often not at 0 V. The most common approach for removing offsets in the data is to subtract the average of the baseline period before the TMS pulse (baseline correction), however, other approaches include subtracting the average of the entire epoch (demeaning the data), subtracting a linear or polynomial function fit from the epoch (detrending the data), or applying a high-pass filter to remove the low-frequency aspects of the data including any offsets. While demeaning and detrending based on the full trial are advisable before calculating time-frequency representations to prevent power from slow frequencies and DC offsets 'bleed' into other frequency bins [247], they are typically discouraged for ERP and therefore TEP analyses. Care should also be taken when demeaning or detrending the data if the TMS pulse/muscle/motion artifact is still present as the large amplitude deflections can influence the average, or the model fit to the data. In addition, the TEPs can be asymmetric and DC offsets may be introduced by the TMS pulse, so detrending may introduce spurious trends in the post-TMS period.

6.2.6. Dealing with large amplitude artifacts

High-amplitude artifacts can have a detrimental effect on temporal filters, by generating ringing artifacts; and on blind source separation approaches like ICA, by biasing the spatial weightings of neuronal components.

Several approaches have been developed to suppress electrode polarization, decay, and TMS-evoked muscle artifacts, and to recover the underlying neuronal signals [213]. One approach is to fit a model representing the artifact to the signal and then subtract the best fit of the model from the data. To fit the decay artifact, linear models, single and double exponential models, adaptive algorithms which select the best fit between linear and exponential models, and biophysical models of the skin/electrode interface (second-order power-law) have been used [82,156,189]. Another approach is to use blind source separation algorithms such as ICA or PCA to separate the EEG signal into different components based on temporal or statistical relationships within the data. The signal is then reconstructed after removing components thought to represent the artifacts. As the amplitude, time-locked nature, and spatial overlap of these artifacts can violate (or at least weaken) some of the assumptions of common ICA and PCA methods, several approaches have been suggested specifically for TMS–EEG data. Some examples include the enhanced deflation method (EDM) of ICA [200], PCA suppression [203], mean-subtracted ICA, momentary-uncorrelated component analysis (MUCA) [240], signal space projection [234], signal space projection with source informed reconstruction (SSP-SIR) [218], the SOUND [221], etc. See **Section 6.3** for a complete list of artifact removal methods.

One of the debated questions in the field is whether ICA or PCA should be used to clean the data. In PCA, the components are set to be uncorrelated, but the decomposition by uncorrelatedness is not unique, so the PCA solution is to some extent arbitrary. ICA on the contrary aims to decompose the EEG data into unique components (artifactual and neural) that are independent. In practice, PCA is useful in giving a set of topographies defining a subspace within which the artifacts are estimated to lie. However, this same subspace also contains neural data, and PCA does not provide any spatial filters that can differentiate the pure artifact signals from the whole data. ICA does yield spatial filters in the form of the demixing matrix, which could give ICA an advantage over PCA. The downside is that the ICA assumptions are rather strict: in addition to independence, the data should be stationary (non-time-dependent), the number of components should stay small (in practice, the same or lower as the data dimensionality, often around 30–40), and the physical component-generation for each component should stay the same for producing a fixed topography. These assumptions are violated by many TMS-evoked artifacts, which can bias the ICA results. Of note, to date we do not know which artifacts are compatible with the ICA assumptions. A significant practical problem is that, currently, we have no tools to test for the goodness of either ICA or PCA in cleaning TEPs, i.e., we lack the ground-truth to assess to what extent neural responses are preserved and artifactual signals removed. These assumptions are violated by many TMS-evoked artifacts, which can bias the ICA results. A significant practical problem is that currently, we have no tools to test for the goodness of either ICA or PCA in cleaning TEPs, i.e., we have no ground-truth to assess to what extent neural responses are preserved and artifactual signals removed.

6.2.7. Dealing with auditory and somatosensory evoked responses (peripheral-evoked potentials-PEPs) in the TMS–EEG

Some of the offline approaches presented in the previous section have been suggested for dealing with PEPs, which include both somatosensory and auditory responses. These approaches include subtracting or regressing a sensory control condition from the TEPs [209], removing components representing PEPs using ICA (at least for the auditory component, [36,222]), and using a variant of SSP-SIR with a sensory control condition [223] (see **Section 3.5** for a full discussion on these issues).

Some of these methods can be applied within the TMS–EEG cleaning pipeline (e.g., ICA), while others necessitate a separate step after the cleaning pipeline and may also require the acquisition of data for an experimental control condition.

6.2.8. Temporal filtering

Temporal filters (low-pass, band-pass, and band-stop "Notch" filters) should be used only after removing the TMS pulse, decay, and muscle artifacts [187,211,213]. High-pass, low-pass, band-pass, and band-stop filters are often used to remove low-frequency drifts, high-frequency noise, and residual line noise from the EEG signal, respectively. Using standard temporal filtering to remove the TMS-elicited artifacts is not recommended because short-lasting peaks consist of multiple frequencies, making the conventional frequency-based filters inefficient. For instance, using a low-pass filter may attenuate the artifact amplitude, but it simultaneously spreads lower-than-cutoff frequency oscillations around the peak, which is termed ringing [211]. High-pass filtering in the presence of the TMS pulse is also problematic and can lead to slow ringing artifacts around the pulse. Therefore, temporal filtering should only be applied once the TMS pulse artifact has been removed.

6.2.9. Interpolate removed channels

When bad channels are removed, a common practice is to interpolate them. Some approaches consist of using spline interpolation of surrounding channels or related methods. The source-informed reconstruction (SIR) allows for interpolation of the channels based on the cortical current estimates based on the non-contaminated channels [218,224]. Channels can be removed and

interpolated from individual trials as opposed to the entire recording, thereby minimizing data loss. Of note, removing or replacing bad channels reduces the dimensionality of the data, which may impact further analysis, for instance, ICA and source analysis.

6.2.10. Averaging across trials

The TMS-evoked EEG data are aligned to the time-locking event, and the voltages from all EEG trials at a given time point are averaged. In other words, the single-trial EEG waveforms are summed and then divided by the number of trials.

6.2.11. Downsampling the data

TMS–EEG data is often collected at high sampling rates (≥5000 Hz) to minimize interactions between low-pass filters and the TMS pulse artifact. While this approach helps to reduce the length of the TMS pulse artifact, the data files are often large (in the order of GB, although this depends on the length of the recording) causing issues with data storage and processing speeds. Furthermore, such high sampling rates often greatly exceed those required to capture the TEPs which are typically <100 Hz in frequency, thereby requiring a minimum sampling frequency of only 400 Hz to adequately characterize the signal. To reduce file sizes, TMS–EEG data are often 'downsampled' to a lower sampling frequency (e.g., 500 or 1000 Hz). An important preprocessing step prior to downsampling is to apply a low-pass filter at ¼ of the target sampling frequency to avoid aliasing artifacts. Anti-aliasing filters are often automatically applied in downsampling functions (e.g., pop_resample.m in EEGLAB) and can cause ringing artifacts if large deflections are present in the data, such as the TMS pulse artifact. Therefore, downsampling should be applied only after TMS pulse and other large-amplitude artifacts have been minimized/removed from the data.

6.2.11.1. What is the optimal order for performing the above steps when processing TMS–EEG data?. To answer this question, a systematic analysis should be performed where real and simulated "ground-truth" data are used. As we have discussed, every step should be applied with caution. Perhaps, the most important advice is to make sure the next step in the analysis is not *negatively* affected by the previous steps. It is also good practice to check the intermediate results of the data processing before drawing any conclusions.

6.3. Methods for removing artifacts from TMS-evoked EEG

In Section 4, we described the nature of different artifacts and outlined some solutions to avoid or reduce them. Unfortunately, following best practices during TMS–EEG preparation and data acquisition are not always sufficient to deal with the TMS-evoked artifacts. This issue has led to the development of numerous advanced offline artifact removal methods, some of which may also be implemented online. However, many publications lack details about the methods, and in many cases, the methods are difficult to implement. In this section, we review some artifact removal methods. For a more detailed explanation and mathematical framework of these approaches, we refer the readers to the work by Hernandez-Pavon et al. [213].

6.3.1. What is the best artifact removal method?

This is a key topic in the TMS–EEG field that has led to the development of several artifact removal procedures. While we do not have an answer to this question, all methods are efficient to remove the artifacts to some extent, no artifact removal method works perfectly in all situations. In the best-case scenario, different methods may be combined to improve their performance [213]. While several methods have become widely adopted, it is important to note that suppressing high-amplitude artifacts while maintaining the underlying neuronal signal is extremely challenging. Currently, we lack empirical data demonstrating the efficacy of these approaches in recovering neuronal signals, mainly because we do not have a ground-truth signal to benchmark methods against. Therefore, these analytical approaches must be used with extreme caution.

6.3.2. Blind source separation

Blind source separation (BSS) is used to decompose the recorded data into spatial and temporal patterns as given by Eq. (2) without using physical modeling of the signal generating processes. This differs from source localization where the mixing **L** is derived from modeling the geometry and conductivity distribution of the head. Typically, no distinction between source types is made within BSS, so we may simply write $\mathbf{Y} = \mathbf{MS}$. The sources **S** are referred to as components and **M** as the mixing matrix. The decomposition is often performed by setting prior assumptions to **S** by considering the columns in **S** as samples collected from a set of underlying random variables. With TMS–EEG, the most often used prior assumptions are the independence and/or uncorrelatedness of the components. Other possibilities include, for example, sparsity of the components, or finding the smallest number of components capable of explaining the time-locked evoked response.

Since BSS methods do not clarify the origin of the components, after estimating the BSS decomposition terms **M** and **S**, the user needs to classify them into relevant categories. This classification is based on features of **S**, such as power spectrum, and **M**, such as spatial smoothness of the topographies. BSS has proven a practical way of removing artifact components from the data. After detecting the artifact components and collecting their mixings and waveforms into **L** and **S**, respectively, one can erase them simply by subtracting them from the data.

6.3.2.1. Independent component analysis (ICA). ICA is probably the most popular BSS method to remove artifacts from EEG data. ICA has been shown to successfully remove a wide variety of artifacts such as blinks, eye movements, muscle activity, heartbeats, and electrical line noise [225].

ICA is a data-driven method that looks for statistically independent components that are non-Gaussian [226,227]. In EEG, the electrodes or sensors record a mixture of electrical responses from neuronal sources in the brain and spurious activity such as artifacts. Then ICA, in principle, can be used to identify components that represent artifacts based on their topographies, time courses, and sample distribution. Components representing artifacts can then be subtracted from the data [225].

In TMS–EEG, ICA has been widely used to remove artifacts of moderate size [228], and strong muscle artifacts after stimulating lateral (e.g., Broca's and Wernicke's areas) and frontal areas of the brain [200]. One approach is to run a two-step ICA on the TMS-evoked EEG data [36,222,229]. In the two-step ICA approach, the first round of ICA is used to remove electrode polarization/TMS-evoked muscle artifacts before a second round of ICA, which is used to identify and suppress other artifacts such as blinks/eye movements and tonic muscle activity. The rationale behind this approach is to optimize the second round of ICA by first suppressing high-amplitude signals, which can result in suboptimal ICA performance, particularly for neuronal signals. In contrast, other pipelines use one round of ICA to suppress all artifact types. It remains unclear how beneficial the two-step approach is in practice. Of note, the number of independent components (ICs) cannot be higher than the rank of the data matrix because the ICA outcome

will not be reliable. This is important to consider when using the two-step ICA approach or after bad channels are removed, as these steps will lower the rank of the data [213].

6.3.2.2. Methods based on PCA. PCA is a method that can be used to reduce the dimensionality of the EEG data, for instance, high-dimensional data can be projected to a lower-dimensional subspace by assuming that the components that account for a relatively large proportion of variance reflect true signals, whereas components that account for relatively little variance reflect artifacts or noise [230].

In TMS–EEG, PCA has been used to remove or suppress TMS-induced artifacts. However, in contrast to the belief that components with little variance reflect artifacts, in TMS–EEG data the first PCs with larger variance have shown to represent muscle artifacts [200,203,231]. Based on that finding, one approach consists in rescaling the artifacts to the size of the brain signals by suppressing the PCs that represent artifacts [203]. Scaling down the artifact directions rather than removing them completely has shown to be beneficial. This method can be applied directly to suppress artifacts from TMS–EEG data [232] but also, as a preprocessing step before ICA [203]. For instance, muscle artifacts are often so large that they may distort the separation of the data to IC and the neuronal components can be affected. Thus, suppressing the largest PCs before ICA can improve ICA performance [203]. Another approach is to use PCA to project out the first PCs with a larger variance to remove the magnetic pulse and muscle artifacts [231].

6.3.3. Methods based on signal space projection (SSP)

Signal-space projection (SSP) is a method for data cleaning in the spatial domain [233]. SSP can be used to estimate the artifact topographies and project them out from the data. As seen in Eq. (2), both the neuronal and artifact signals consist of time-invariant topographies (the column vectors of matrices **L**) and the corresponding time-varying amplitudes (the row vectors of matrices **S**). Even though the artifactual and neuronal signals might heavily overlap in time and frequency domains, there might still be time intervals or frequency ranges that contain only artifact signals. The idea of SSP is to utilize these segments of data to estimate the artifact topographies to be rejected. For instance, the TMS-evoked muscle artifacts overlap in time and frequency with the early cortical responses to TMS. However, muscle activity is seen in EEG also at high frequencies (above 100 Hz), which is atypical for neuronal signals. Thus, SSP can estimate the muscle-artifact topographies from the high-pass filtered data and project them out from the whole TMS–EEG dataset [234]. The key assumption here is that both the high- and low-frequency components of muscle artifacts have similar spatial topographies. One disadvantage of SSP is its tendency to distort the data spatially. Once the artifact topographies are projected out, the rows of the cleaned data do not directly correspond to any of the original physical EEG electrodes. Instead, each of the data rows corresponds to virtual EEG channels that are sensitive to neuronal EEG signals but insensitive to the suppressed artifacts. In addition, projecting out topographies lowers the rank of the data. The distortional effects can be, however, taken into account with SIR (see **Section 6.3.5** for details).

In TMS–EEG, SSP has been used to suppress both the TMS-induced muscle artifacts [218,234] and the TMS-pulse related sensory inputs [223]. These approaches have been implemented in the open-source TESA toolbox [187,235].

6.3.4. Source model-based methods

The neuronal EEG signals have different electromagnetic generators than the various artifact- and noise components. Most noise and artifacts originate from extracranial sources and thus can show different spatial features. This is depicted by Eq. (2), which shows that each signal category has its own lead field or mixing matrices (**L**). This characteristic low spatial resolution of neuronal signals can also be exploited in TMS–EEG data analysis to separate the neuronal components from the various disturbances. With the help of mathematical and numerical tools (e.g., Refs. [236,237]), and electromagnetic theory [238], we can forward model the topographies generated by different cortical sources and calculate the lead field (Eq. (2)). In short, the source-model-based methods could be defined as techniques that use the lead field and consecutive inverse and forward computation steps to separate artifact signals from the data. One of the first attempts was made by Litvak et al. [189], who constructed a model matrix containing sets of representative artifactual and neuronal topographies, the former being estimated from the data and the latter using forward modeling. By solving the inverse problem of the TMS–EEG data using the constructed model matrix, the TEPs were separated into neuronal and artifactual components. The artifact signals were finally subtracted from the original data.

SSP–SIR belongs to source model-based methods and can be used to project out artifacts and interpolate removed channels [218]. SSP–SIR is an extension of the previously described SSP. The idea of the SIR step is to extrapolate the removed signal dimensions, and hence recover the neuronal topographies distorted by SSP, using consecutive inverse and forward estimations. Another method that has proven to be useful for TMS–EEG applications is the SOUND algorithm. SOUND finds a spatial filter to cancel out spurious EEG signals such as electrode-polarization, line-noise, and electrode-movement artifacts, which are not likely to originate from intracranial postsynaptic currents [221]. Recently, SOUND has successfully been tested for real-time TMS–EEG data [239]. The spatial filter was updated on a parallel process, while the streaming data was cleaned instantaneously with the most recent SOUND filter.

6.3.5. Modified ICA and BSS

TMS-evoked EEG signals are time-dependent, which is highlighted by the fact that the averaged EEG trials show a time-varying mean. In addition, induced oscillations are known to show synchronization (increase in power) or desynchronization (decrease) patterns changing as a function of time and frequency. In statistical terms, it is said that TMS–EEG data are *non-stationary* because the statistical properties (e.g., mean and variance) are different at different times.

Commonly, the BSS approaches assume that the input data are stationary and can yield biased estimates when this assumption is not met by the data, but it is also possible to design BSS which makes use of the changing properties of the data. If components are active at overlapping time windows, ICA may not be capable of accurately separating them since they easily become correlated and dependent (see Ref. [213] for examples). Metsomaa et al. [240] illustrated how simple preprocessing of the data makes the data mean-independent, meaning that the mean of the underlying components cannot be predicted from other components. Mean-independence is sufficient for FastICA and several other ICA methods to separate the signals even if their waveforms tend to activate simultaneously [227]. In practice, the artifact amplitude is also significantly reduced by mean subtraction [240], which results in numerically stable solutions. The requirement is that the average data containing phase-locked activity constitutes roughly the same dominant components as the single-trial data.

Rather than assuming independence, one may make the assumption that the components to be separated are uncorrelated. Performing BSS only based on the assumption of uncorrelatedness is not a sufficient criterion for getting a unique decomposition.

Because of non-stationarity, we can set the assumption of uncorrelatedness separately at each time point, which gives us enough criteria to perform component separation based on uncorrelatedness only. Metsomaa et al. [241], developed MUCA to uncover components that are uncorrelated at each selected time point (or time window) after TMS. Additionally, the variances of the components (powers) need to change over time points. The benefit of using uncorrelated components rather than independent components in BSS is that ICA easily overfits outliers and sparsely occurring activity, making the decomposition inaccurate.

In practice, based on the pre-requisites of MUCA, it is especially suitable for uncovering induced oscillations where the power of neuronal oscillators changes with time relative to the TMS onset. MUCA does not require filtering, but band-pass filtering may be useful if one is interested in a particular frequency band. Both MUCA [241] and the mean-subtraction approach [240] are suitable for studying trial-to-trial variability in the TEPs/induced oscillations because the deterministic (averaged) TEP is not relevant for such interpretations.

7. Toolboxes for TMS–EEG data analysis

Different toolboxes have been developed to facilitate the analysis of TMS-evoked EEG data: FieldTrip [242], TMSEEG [243], TMS–EEG signal analyzer (TESA) [187], Automated aRTIfact rejection for single-pulse TMS–EEG Data (ARTIST) [244], and The Brain Electrophysiological recording and STimulation (BEST) [216]. There has also been an interest in comparing the impact of the pipelines used in some of the previous toolboxes on the TMS–EEG signals [112]. In this section, we present general aspects of different toolboxes and their content.

7.1. FieldTrip

While the FieldTrip toolbox for MATLAB ([242]; www.fieldtriptoolbox.org) does not provide a GUI nor a fixed predefined pipeline for TMS–EEG analysis, according to its philosophy, a series of MATLAB functions accompanied by a detailed tutorial and example datasets are made available online (*www.fieldtriptoolbox.org/tutorial/tms-eeg*) to support TMS–EEG artifact removal (including pulse artifact interpolation and ICA-based removal of muscle/decay artifacts) and analyses (TEPs, TFRs, global mean field power, GMFP) according to the pipeline published by Herring et al. [49].

7.2. TMSEEG

The TMSEEG toolbox is a plug-in implemented within EEGLAB on the MATLAB platform [243]. This toolbox includes ten steps divided into preprocessing, removing different artifacts with two ICA steps, filtering, and data visualization. In particular, the toolbox allows removing the TMS artifact by removing the segment of the data where this artifact is present. Then the bad channels and trials can be removed, and thereafter two ICA steps can be applied. The first ICA step aims to remove the TMS decay artifact, whereas the second step may remove residual TMS and general EEG artifacts. TMSEEG makes use of FastICA [227]. The code for TMSEEG is available at http://www.tmseeg.com/downloads/.

7.3. TESA

The TESA toolbox (TMS–EEG signal analyzer) [187] is also a plug-in implemented within the popular EEG analysis toolbox EEGLAB [245] on the MATLAB platform. The overarching aim of TESA is to provide a standardized library of methods used in TMS–EEG research, thereby improving the transparency and reproducibility of TMS–EEG analysis across the field. TESA follows the modular format of EEGLAB, allowing the flexible design of analysis pipelines and integration with existing EEGLAB functions. As such, TESA does not advocate for any particular pipeline but allows users to easily design and compare different analysis approaches.

TESA includes a broad range of functions coding different analysis steps, including finding the TMS pulse artifact; removing and interpolating data around the TMS pulse and recharge artifacts; suppressing electrode polarization and TMS-evoked muscle activity artifacts (FastICA, EDM, PCA, SSP-SIR, SOUND, linear and exponential models); region-of-interest, peak and amplitude analysis of TEPs; and basic TEP visualization [187,200,203,235]. TESA also includes heuristic methods for classifying ICA components based on different artifact signal features. Each analysis function is represented across two levels: a base function containing the relevant analysis code, and a 'pop' function that launches a GUI window, allowing users to manually modify input parameters without interacting with the MATLAB command line. Users can generate the command line function for a given analysis method from the GUI windows using the EEGLAB history feature and then use the command line functions to build analysis pipelines as MATLAB script files. The GUI implementation of EEGLAB is particularly helpful for users not familiar with coding and ensures that methods are available and accessible to all members of the TMS–EEG community regardless of their background and skill set.

The process of converting pipelines to scripts helps to standardize and automate analysis across data sets for a given project, minimizing the possibility of errors associated with manual point-and-click analysis. Importantly, these pipeline scripts can be published alongside manuscripts (e.g., through platforms like GitHub or the open science framework), providing an easy way to ensure the reproducibility of published analyses. The code for TESA is available at: *https://github.com/nigelrogasch/TESA/releases*. TESA is also supported by an open-access online book, the TESA user manual, which details how to use TESA and considerations for developing TMS–EEG analysis pipelines: *https://nigelrogasch.gitbook.io/tesa-user-manual/*. With the help of the TMS–EEG community, it is hoped the TESA library will continue to grow as new and improved methods become available.

7.4. Automated aRTIfact rejection for Single-pulse TMS–EEG data (ARTIST)

The main difference between ARTIST and the previous toolboxes is that ARTIST is based on a fully automated algorithm for single-pulse TMS (spTMS)–EEG artifact rejection [244]. The algorithm implemented in ARTIST decomposes the spTMS–EEG data into ICs, and then trains a pattern classifier to automatically identify artifact components based on knowledge of the spatio-temporal profile of both neuronal and artifactual activities. ARTIST consists of three stages, each aimed at removing specific types of artifacts. The first stage removes large-amplitude TMS-related artifacts from the continuous data (removes DC drift, removes and interpolates the TMS pulse artifact, downsamples, and removes the decay artifacts with a one-step ICA). The second stage band-pass filters the continuous data to remove the AC line noise and high-frequency noise and then rejects bad epochs and channels from the epoched data. The third stage removes the remaining artifacts (for instance, the residual decay artifacts, ocular artifacts, ECG artifact, and persistent EMG artifact with a second ICA step) from the epoched data after the data are re-referenced to the common average and baseline corrected. ARTIST applies a two-step ICA; the ICA algorithm is based on Infomax [226]. The code for ARTIST is available at http://etkinlab.stanford.edu/toolboxes/ARTIST/.

7.5. BEST toolbox

The Brain Electrophysiological recording and STimulation (BEST) toolbox (www.best-toolbox.org) is an open-source MATLAB toolbox with GUI [216], which enables the user to easily design, save/load, run, and online analyze multi-protocol/multi-session experiments involving a variety of brain stimulation techniques, such as TMS, TES and also transcranial ultrasound stimulation. It interfaces with many recording and stimulation devices and can online analyze and display the input signals from EMG and EEG and change TMS parameters on the fly (via the MAGIC toolbox, [246]), thereby facilitating real-time applications. Besides several modules for conducting MEP measurements of all kinds (such as motor hotspot search, threshold hunting, MEP measurements, dose-response curves, as well as paired-pulse and double-coil protocols), the BEST toolbox also supports TEP hotspot search and TEP measurements by providing online graphical feedback for re-referenced EEG signals (also lead fields for arbitrary spatial filters can be defined), incremental condition-wise time-locked TEP averages and topographical maps of selected TEP components. Future releases are planned to also provide real-time artifact rejection methods. The BEST toolbox does not provide a built-in TMS–EEG artifact correction pipeline but can interact with all MATLAB-based pipelines or toolboxes. The internal data format is based on FieldTrip.

8. Conclusion and future directions

In this article, we have reviewed the state of the art of TMS–EEG technique. We have covered TMS–EEG hardware, preparation, data collection, and analysis. The TMS–EEG field is growing rapidly, and we have identified and discussed the challenges of the technique. Our goal is to provide a set of recommendations when possible or to provide alternatives for cases where standard practices have not been developed. We hope this article will be useful to both established TMS–EEG researchers and newcomers in the field and that it will promote the joint discussion of key issues and a collaborative effort to find effective solutions.

CRediT author contribution statement

Julio C. Hernandez-Pavon: Conceptualization; Data curation; Formal analysis; Investigation; Methodology; Project administration; Resources; Supervision; Validation; Visualization; Roles/Writing - original draft; Writing - review & editing; **Domenica Veniero:** Conceptualization; Data curation; Formal analysis; Investigation; Methodology; Project administration; Resources; Supervision; Validation; Visualization; Roles/Writing - original draft; Writing - review & editing; **Til Ole Bergmann, Paolo Belardinelli, Marta Bortoletto, Silvia Casarotto, Elias Casula, Faranak Farzan, Matteo Fecchio, Petro Julkunen, Elisa Kallioniemi, Pantelis Lioumis, Johanna Metsomaa, Carlo Miniussi, Tuomas P. Mutanen, Lorenzo Rocchi, Nigel C. Rogasch, Mouhsin M. Shafi, Hartwig R. Siebner, Gregor Thut, Christoph Zrenner, Ulf Ziemann:** Investigation; Methodology; Writing - review & editing; **Risto J. Ilmoniemi:** Funding acquisition; Investigation; Methodology; Writing - review & editing.

Declaration of competing interest

The authors declare the following financial interests/personal relationships which may be considered as potential competing interests: PJ has received consulting fees and shares a patent with Nexstim Oyj. PL has received consulting fees from Nexstim Oyj. HRS has received honoraria as speaker from Sanofi Genzyme, Denmark, Lundbeck AS, Denmark, and Novartis, Denmark, as consultant from Sanofi Genzyme, Denmark, Lophora, Denmark, and Lundbeck AS, Denmark, and as editor-in-chief (Neuroimage Clinical) and senior editor (NeuroImage) from Elsevier Publishers, Amsterdam, The Netherlands. He has received royalties as book editor from Springer Publishers, Stuttgart, Germany and from Gyldendal Publishers, Copenhagen, Denmark. TPM has successfully applied for funding for a collaborative research project (project not started at the time of the submission) with Bittium Biosignals Oy (Kuopio, Finland). SC is advisor and share-holder of Intrinsic Power, a spinf-off of the University of Milan.

Acknowledgments

JCHP and RJI want to dedicate this work to the memory of Prof. Jukka Sarvas, one of the most beautiful minds and humble hearts that have existed in this world. HRS holds a 5-year professorship in precision medicine at the Faculty of Health Sciences and Medicine, University of Copenhagen which is sponsored by the Lundbeck Foundation (Grant Nr. R186-2015-2138). TPM has been supported by the Academy of Finland (Grant No. 321631).

Appendix A. Supplementary data

Supplementary data to this article can be found online at https://doi.org/10.1016/j.brs.2023.02.009.

References

[1] Barker A, Jalinous R, Freeston I. Non-invasive magnetic stimulation of human motor cortex. Lancet 1985;1(8437):1106–7.
[2] Cracco R, Amassian V, Maccabee P, Cracco J. Comparison of human transcallosal responses evoked by magnetic coil and electrical stimulation. Electroencephalogr Clin Neurophysiol 1989;74:417–24.
[3] Amassian V, Cracco R, Maccabee P, Cracco J. Cerebello-frontal cortical projections in humans studied with the magnetic coil. Electroencephalogr Clin Neurophysiol 1992;85(4):265–72.
[4] Ilmoniemi R, Virtanen J, Ruohonen J, Karhu J, Aronen H, Näätänen R, et al. Neuronal responses to magnetic stimulation reveal cortical reactivity and connectivity. Neuroreport 1997;8:3537–40.
[5] Tremblay S, Rogasch N, Premoli I, Blumberger D, Casarotto S, Chen R, et al. Clinical utility and prospective of TMS–EEG. Clin Neurophysiol 2019;130(5):802–44.
[6] Ridding M, Rothwell J. Is there a future for therapeutic use of transcranial magnetic stimulation? Nat Rev Neurosci 2007;8(7):559–67.
[7] Ilmoniemi R, Ruohonen J, Virtanen J, Aronen H, Karhu J. EEG responses evoked by transcranial magnetic stimulation. Electroencephalogr Clin Neurophysiol Suppl 1999;51:22–9.
[8] Siebner HR, Funke K, Aberra AS, Antal A, Bestmann S, Chen R, et al. Transcranial magnetic stimulation of the brain: what is stimulated? - a consensus and critical position paper. Clin Neurophysiol 2022;140:59–97.
[9] Maccabee P, Amassian V, Eberle L, Cracco R. Magnetic coil stimulation of straight and bent amphibian and mammalian peripheral nerve in vitro: locus of excitation. J Physiol 1993;460:201–19.
[10] Ruohonen J. Chapter 1 background physics for magnetic stimulation. Supplements to clinical neurophysiology transcranial magnetic stimulation and transcranial direct current stimulation, proceedings of the 2nd international transcranial magnetic stimulation (TMS) and transcranial direct current stimulation (tDCS). Symposium 2003;56:3–12.
[11] Deng Z, Lisanby S, Peterchev A. Electric field depth-focality tradeoff in transcranial magnetic stimulation: simulation comparison of 50 coil designs. Brain Stimul 2013;6(1):1–13.
[12] Ilmoniemi R, Ruohonen J, Karhu J. Transcranial magnetic stimulation–a new tool for functional imaging of the brain. Crit Rev Biomed Eng 1999;27(3–5):241–84.
[13] Romero M, Davare M, Armendariz M, Janssen P. Neural effects of transcranial magnetic stimulation at the single-cell level. Nat Commun 2019;10(2642):1–11.
[14] Di Lazzaro V, Ziemann U. The contribution of transcranial magnetic stimulation in the functional evaluation of microcircuits in human motor cortex. Front Neural Circ 2013;7:18.
[15] Bergmann TO, Hartwigsen G. Inferring causality from noninvasive brain stimulation in cognitive neuroscience. J Cognit Neurosci 2021;33(2):195–225.
[16] Baillet S, Mosher J, Leahy R. Electromagnetic brain mapping. IEEE Signal Process Mag 2001;18(6):14–30.

[17] Bergmann T, Karabanov A, Hartwigsen G, Thielscher A, Siebner H. Combining non-invasive transcranial brain stimulation with neuroimaging and electrophysiology: current approaches and future perspectives. Neuroimage 2016;140:4–19.
[18] Hallett M, Di Iorio R, Rossini P, Park J, Chen R, Celnik P, et al. Contribution of transcranial magnetic stimulation to assessment of brain connectivity and networks. Clin Neurophysiol 2017;128(11):2125–39.
[19] Siebner H, Bergmann T, Bestmann S, Massimini M, Johansen-Berg H, Mochizuki H, et al. Consensus paper: combining transcranial stimulation with neuroimaging. Brain Stimul 2009;2(2):58–80.
[20] Berger H. Uber das Elektroenkephalogramm des Menschen (On the electroencephalogram of man). Arch Psychiatr Nervenkr 1929;87:527–70.
[21] Cohen M. Where does EEG come from and what does it mean? Trends Neurosci 2017;40(4):208–18.
[22] Schomer D, da Silva F. Niedermeyer's electroencephalography: basic principles, clinical applications, and related fields. 2018.
[23] Ilmoniemi R, Sarvas J. Brain signals physics and mathematics of MEG and EEG. The MIT Press; 2019.
[24] Okada Y, Wu J, Kyuhou S. Genesis of MEG signals in a mammalian CNS structure. Electroencephalogr Clin Neurophysiol 1997;103:474–85.
[25] de Munck J, Vijn P, Lopez da Silva F. A random dipole model for spontaneous brain activity. IEEE Trans Biomed Eng 1992;39(8):791–804.
[26] Ilmoniemi R. Neuromagnetism : theory, techniques, and measurements department of technical physics. Espoo, Finland: Helsinki University of Technology; 1985.
[27] Miniussi C, Thut G. Combining TMS and EEG offers new prospects in cognitive neuroscience. Brain Topogr 2010;22(4):249–56.
[28] Ilmoniemi R, Kicić D. Methodology for combined TMS and EEG. Brain Topogr 2010;22(4):233–48.
[29] Bortoletto M, Bonzano L, Zazio A, Ferrari C, Pedullà L, Gasparotti R, et al. Asymmetric transcallosal conduction delay leads to finer bimanual coordination. Brain Stimul 2021;14(2):379–88.
[30] Kallioniemi E, Saari J, Ferreri F, Määttä S. TMS-EEG responses across the lifespan: measurement, methods for characterisation and identified responses. J Neurosci Methods 2022;366(109430):1–19.
[31] Luck S. An introduction to the event-related potential technique. second ed. 2014. Second Edition.
[32] Lioumis P, Kičić D, Savolainen P, Mäkelä J, Kähkönen S. Reproducibility of TMS-Evoked EEG responses. Hum Brain Mapp 2009;30(4):1387–96.
[33] Kerwin L, Keller C, Wu W, Narayan M, Etkin A. Test-retest reliability of transcranial magnetic stimulation EEG evoked potentials. Brain Stimul 2018;11(3):536–44.
[34] Casarotto S, Fecchio M, Rosanova M, Varone G, D'Ambrosio S, Sarasso S, et al. The rt-TEP tool: real-time visualization of TMS-Evoked Potential to maximize cortical activation and minimize artifacts. J Neurosci Methods 2022;370:109486.
[35] Komssi S, Kähkönen S, Ilmoniemi R. The effect of stimulus intensity on brain responses evoked by transcranial magnetic stimulation. Hum Brain Mapp 2004;21:154–64.
[36] Rogasch NC, Thomson RH, Farzan F, Fitzgibbon BM, Bailey NW, Hernandez-Pavon JC, et al. Removing artifacts from TMS-EEG recordings using independent component analysis: importance for assessing prefrontal cortex network properties. Neuroimage 2014;101:425–39.
[37] Bonato C, Miniussi C, Rossini P. Transcranial magnetic stimulation and cortical evoked potentials: a TMS/EEG co-registration study. Clin Neurophysiol 2006;117(8):1699–707.
[38] Rocchi L, Di Santo A, Brown K, Ibáñez J, Casula E, Rawji V, et al. Disentangling EEG responses to TMS due to cortical and peripheral activations. Brain Stimul 2021;14(1):4–18.
[39] Belardinelli P, König F, Liang C, Premoli I, Desideri D, Müller-Dahlhaus F, et al. TMS-EEG signatures of glutamatergic neurotransmission in human cortex. Sci Rep 2021;11(1):1–14.
[40] Nikulin V, Kičić D, Kähkönen S, Ilmoniemi R. Modulation of electroencephalographic responses to transcranial magnetic stimulation: evidence for changes in cortical excitability related to movement. Eur J Neurosci 2003;18(5):1206–12.
[41] Massimini M, Ferrarelli F, Huber R, Esser S, Singh H, Tononi G. Breakdown of cortical effective connectivity during sleep. Science 2005;309(5744):2228–32.
[42] Sarasso S, Boly M, Napolitani M, Gosseries O, Charland-Verville V, Casarotto S, et al. Consciousness and complexity during unresponsiveness induced by propofol, xenon, and ketamine. Curr Biol 2015;25(23):3099–105.
[43] Shafi M, Vernet M, Klooster D, Chu C, Boric K, Barnard M, et al. Physiological consequences of abnormal connectivity in a developmental epilepsy. Ann Neurol 2015;77(3):487–503.
[44] Fox P, Narayana S, Tandon N, Fox S, Sandoval H, Kochunov P, et al. Intensity modulation of TMS-induced cortical excitation: primary motor cortex. Hum Brain Mapp 2006;27:478–87.
[45] Saari J, Kallioniemi E, Tarvainen M, Julkunen P. Oscillatory TMS-EEG-responses as a measure of the cortical excitability threshold. IEEE Trans Neural Syst Rehabil Eng 2018;26(2):383–91.
[46] Rosanova M, Casali A, Bellina V, Resta F, Mariotti M, Massimini M. Natural frequencies of human corticothalamic circuits. J Neurosci 2009;29(24):7679–85.
[47] Thut G, Miniussi C, Gross J. The functional importance of rhythmic activity in the brain. Curr Biol 2012;22(16):R658–63.
[48] Vallesi A, Del Felice A, Capizzi M, Tafuro A, Formaggio E, Bisiacchi P, et al. Natural oscillation frequencies in the two lateral prefrontal cortices induced by Transcranial Magnetic Stimulation. Neuroimage 2021;227:117655.
[49] Herring JD, Thut G, Jensen O, Bergmann TO. Attention modulates TMS-locked alpha oscillations in the visual cortex. J Neurosci 2015;35(43):14435–47.
[50] Veniero D, Gross J, Morand S, Duecker F, Sack AT, Thut G. Top-down control of visual cortex by the frontal eye fields through oscillatory realignment. Nat Commun 2021;12(1):1757.
[51] David O., Kiebel S.J., Harrison L.M., Mattout J., Kilner J.M., Friston K.J. Dynamic causal modeling of evoked responses in EEG and MEG. Neuroimage 2006;30(4)1255–1272.
[52] Premoli I, Bergmann T, Fecchio M, Rosanova M, Biondi A, Belardinelli P, et al. The impact of GABAergic drugs on TMS-induced brain oscillations in human motor cortex. Neuroimage 2017;163:1–12.
[53] Thut G, Bergmann TO, Frohlich F, Soekadar SR, Brittain JS, Valero-Cabre A, et al. Guiding transcranial brain stimulation by EEG/MEG to interact with ongoing brain activity and associated functions: a position paper. Clin Neurophysiol 2017;128(5):843–57.
[54] Pellicciari MC, Veniero D, Miniussi C. Characterizing the cortical oscillatory response to TMS pulse. Front Cell Neurosci 2017;11:38.
[55] Casarotto S, Romero Lauro L, Bellina V, Casali A, Rosanova M, Pigorini A, et al. EEG responses to TMS are sensitive to changes in the perturbation parameters and repeatable over time. PLoS One 2010;5(4):e10281.
[56] Gosseries O, Sarasso S, Casarotto S, Boly M, Schnakers C, Napolitani M, et al. On the cerebral origin of EEG responses to TMS: insights from severe cortical lesions. Brain Stimul 2015;8(1):142–9.
[57] Rossi S, Antal A, Bestmann S, Bikson M, Brewer C, Brockmöller J, et al. Safety and recommendations for TMS use in healthy subjects and patient populations, with updates on training, ethical and regulatory issues: expert Guidelines. Clin Neurophysiol 2021;132(1):269–306.
[58] Deng Z, Lisanby S, Peterchev A. Coil design considerations for deep transcranial magnetic stimulation. Clin Neurophysiol 2014;125(6):1202–12.
[59] Ueno S, Tashiro T, Harada K. Localized stimulation of neural tissue in the brain by means of a paired configuration of time-varying magnetic fields. J App Phys 1988;64:5862–4.
[60] Fernandez L, Biabani M, Do M, Opie G, Hill A, Barham M, et al. Assessing cerebellar-cortical connectivity using concurrent TMS-EEG: a feasibility study. J Neurophysiol 2021;125(5):1768–87.
[61] Koponen L, Nieminen J, Ilmoniemi R. Multi-locus transcranial magnetic stimulation-theory and implementation. Brain Stimul 2018;11(4):849–55.
[62] Nieminen JO, Sinisalo H, Souza VH, Malmi M, Yuryev M, Tervo AE, et al. Multi-locus transcranial magnetic stimulation system for electronically targeted brain stimulation. Brain Stimul 2022;15(1):116–24.
[63] Souza VH, Nieminen JO, Tugin S, Koponen LM, Baffa O, Ilmoniemi RJ. TMS with fast and accurate electronic control: measuring the orientation sensitivity of corticomotor pathways. Brain Stimul 2022;15(2):306–15.
[64] Tervo AE, Nieminen JO, Lioumis P, Metsomaa J, Souza VH, Sinisalo H, et al. Closed-loop optimization of transcranial magnetic stimulation with electroencephalography feedback. Brain Stimul 2022;15(2):523–31.
[65] Sommer M, Alfaro A, Rummel M, Speck S, Lang N, Tings T, et al. Half sine, monophasic and biphasic transcranial magnetic stimulation of the human motor cortex. Clin Neurophysiol 2006;117(4):838–44.
[66] Jung N, Delvendahl I, Pechmann A, Gleich B, Gattinger N, Siebner H, et al. Transcranial magnetic stimulation with a half-sine wave pulse elicits direction-specific effects in human motor cortex. BMC Neurosci 2012;13(139):1–9.
[67] Delvendahl I, Gattinger N, Berger T, Gleich B, Siebner H, Mall V. The role of pulse shape in motor cortex transcranial magnetic stimulation using full-sine stimuli. PLoS One 2014;9(12):e115247.
[68] Delvendahl I, Lindemann H, Jung N, Pechmann A, Siebner H, Mall V. Influence of waveform and current direction on short-interval intracortical facilitation: a paired-pulse TMS study. Brain Stimul 2014;7(1):49–58.
[69] Groppa S, Oliviero A, Eisen A, Quartarone A, Cohen L, Mall V, et al. A practical guide to diagnostic transcranial magnetic stimulation: report of an IFCN committee. Clin Neurophysiol 2012;23(5). 858-582.
[70] Funke K. Transcranial magnetic stimulation of rodents: repetitive transcranial magnetic stimulation—a noninvasive way to induce neural plasticity in vivo and in vitro. In: Manahan-Vaughan D, editor. Handbook of behavioral neuroscience. Elsevier; 2018. p. 365–87.
[71] Rossini P, Burke D, Chen R, Cohen L, Z D, Di Iorio R, et al. Non-invasive electrical and magnetic stimulation of the brain, spinal cord, roots and peripheral nerves: basic principles and procedures for routine clinical and research application. An updated report from an I.F.C.N. Committee. Clin Neurophysiol 2015;26(6):1071–107.
[72] Kammer T, Beck S, Thielscher A, Laubis-Herrmann U, Topka H. Motor thresholds in humans: a transcranial magnetic stimulation study comparing different pulse waveforms, current directions and stimulator types. Clin Neurophysiol 2001;112(2):250–8.
[73] Mills K, Boniface S, Schubert M. Magnetic brain stimulation with a double coil: the importance of coil orientation. Electroencephalogr Clin Neurophysiol 1992;85:17–21.

[74] Corthout E, Barker A, Cowey A. Transcranial magnetic stimulation: which part of the current waveform causes the stimulation? Exp Brain Res 2001;141(1):128–32.
[75] Mutanen T, Mäki H, Ilmoniemi R. The effect of stimulus parameters on TMS-EEG muscle artifacts. Brain Stimul 2013;6(3):371–6.
[76] Rogasch NC, Thomson RH, Daskalakis ZJ, Fitzgerald PB. Short-latency artifacts associated with concurrent TMS-EEG. Brain Stimul 2013;6(6):868–76.
[77] Veniero D, Bortoletto M, Miniussi C. TMS-EEG co-registration: on TMS-induced artifact. Clin Neurophysiol 2009;120(7):1392–9.
[78] Casula E, Rocchi L, Hannah R, Rothwell J. Effects of pulse width, waveform and current direction in the cortex: a combined cTMS-EEG study. Brain Stimul 2018;11(5):1063–70.
[79] Virtanen J, Ruohonen J, Näätänen R, Ilmoniemi R. Instrumentation for the measurement of electric brain responses to transcranial magnetic stimulation. Med Biol Eng Comput 1999;37(3):322–6.
[80] Iramina I, Maeno T, Nonaka Y, Ueno S. Measurement of evoked electroencephalography induced by transcranial magnetic stimulation. J Appl Phys 2003;93(10):6718–20.
[81] Taylor J, Loo C. Stimulus waveform influences the efficacy of repetitive transcranial magnetic stimulation. J Affect Disord 2007;97(1–3):271–6.
[82] Freche D, Naim-Feil J, Peled A, Levit-Binnun N, Moses E. A quantitative physical model of the TMS-induced discharge artifacts in EEG. PLoS Comput Biol 2018;14(7):1–35.
[83] Bae J, MacFall J, Krishnan K, Payne M, Steffens D, Taylor W. Dorsolateral prefrontal cortex and anterior cingulate cortex white matter alterations in late-life depression. Biol Psychiatr 2006;60(12):1356–63.
[84] Tanner D, Norton JJ, Morgan-Short K, Luck SJ. On high-pass filter artifacts (they're real) and baseline correction (it's a good idea) in ERP/ERMF analysis. J Neurosci Methods 2016;266:166–70.
[85] Varone G, Hussain Z, Sheikh Z, Howard A, Boulila W, Mahmud M, et al. Real-time artifacts reduction during TMS-EEG Co-registration: a comprehensive review on technologies and procedures. Sensors (Basel) 2021;21(637):1–23.
[86] Mancuso M, Sveva V, Cruciani A, Brown K, Ibáñez J, Rawji V, et al. Transcranial evoked potentials can Be reliably recorded with active electrodes. Brain Sci 2021;11(145):1–16.
[87] Ozdemir R, Tadayon E, Boucher P, Momi D, Karakhanyan K, Fox M, et al. Individualized perturbation of the human connectome reveals reproducible biomarkers of network dynamics relevant to cognition. Proc Natl Acad Sci U S A 2020;117(14):8115–25.
[88] Rawji V, Kaczmarczyk I, Rocchi L, Fong PY, Rothwell JC, Sharma N. Preconditioning stimulus intensity alters paired-pulse TMS evoked potentials. Brain Sci 2021;11(3).
[89] Julkunen P, Säisänen L, Sarasti M, Könönen M. Effect of electrode cap on measured cortical motor threshold. J Neurosci Methods 2009;176(2):225–9.
[90] Jasper H. The ten-twenty electrode system of the international federation. Electroencephalogr Clin Neurophysiol 1958;10:371–5.
[91] Iivanainen J, Makinen AJ, Zetter R, Stenroos M, Ilmoniemi RJ, Parkkonen L. Spatial sampling of MEG and EEG based on generalized spatial-frequency analysis and optimal design. Neuroimage 2021;245:118747.
[92] Ryynanen OR, Hyttinen JA, Laarne PH, Malmivuo JA. Effect of electrode density and measurement noise on the spatial resolution of cortical potential distribution. IEEE Trans Biomed Eng 2004;51(9):1547–54.
[93] Michel CM, Brunet D. EEG source imaging: a practical review of the analysis steps. Front Neurol 2019;10:325.
[94] Sohrabpour A, Lu Y, Kankirawatana P, Blount J, Kim H, He B. Effect of EEG electrode number on epileptic source localization in pediatric patients. Clin Neurophysiol 2015;126(3):472–80.
[95] Goldenholz DM, Ahlfors SP, Hamalainen MS, Sharon D, Ishitobi M, Vaina LM, et al. Mapping the signal-to-noise-ratios of cortical sources in magnetoencephalography and electroencephalography. Hum Brain Mapp 2009;30(4):1077–86.
[96] Sack A, Kadosh R, Schuhmann T, Moerel M, Walsh V, Goebel R. Optimizing functional accuracy of TMS in cognitive studies: a comparison of methods. J Cognit Neurosci 2009;21(2):207–21.
[97] Lioumis P, Rosanova M. The role of neuronavigation in TMS-EEG studies: current applications and future perspectives. J Neurosci Methods 2022;380:109677.
[98] Ruohonen J, Karhu J. Navigated transcranial magnetic stimulation. Neurophysiol Clin 2010;40(1):7–17.
[99] Hannula H, Ilmoniemi R. Basic principles of navigated TMS. In: Krieg S, editor. Navigated transcranial magnetic stimulation in neurosurgery. Springer; 2017.
[100] Bashir S, Edwards D, Pascual-Leone A. Neuronavigation increases the physiologic and behavioral effects of low-frequency rTMS of primary motor cortex in healthy subjects. Brain Topogr 2011;24(1):54–64.
[101] Cincotta M, Giovannelli F, Borgheresi A, Balestrieri F, Toscani L, Zaccara G, et al. Optically tracked neuronavigation increases the stability of hand-held focal coil positioning: evidence from "transcranial" magnetic stimulation-induced electrical field measurements. Brain Stimul 2010;3(2):119–23.
[102] Julkunen P, Säisänen L, Danner N, Niskanen E, Hukkanen T, Mervaala E, et al. Comparison of navigated and non-navigated transcranial magnetic stimulation for motor cortex mapping, motor threshold and motor evoked potentials. Neuroimage 2009;44(3):790–5.
[103] Thielscher A, Opitz A, Windhoff M. Impact of the gyral geometry on the electric field induced by transcranial magnetic stimulation. Neuroimage 2011;54(1):234–43.
[104] Thut G, Veniero D, Romei V, Miniussi C, Schyns P, Gross J. Rhythmic TMS causes local entrainment of natural oscillatory signatures. Curr Biol 2011;21(14):1176–85.
[105] Sarvas J. Basic mathematical and electromagnetic concepts of the biomagnetic inverse problem. Phys Med Biol 1987;32(1):11–22.
[106] Nummenmaa A, Stenroos M, Ilmoniemi R, Okada Y, Hämäläinen M, Raij T. Comparison of spherical and anatomically realistic boundary element head models for transcranial magnetic stimulation navigation. Clin Neurophysiol 2013;124(10):1995–2007.
[107] Thielscher A, Antunes A, Saturnino G. Field modeling for transcranial magnetic stimulation: a useful tool to understand the physiological effects of TMS? Annu Int Conf IEEE Eng Med Biol Soc 2015:222–5.
[108] de Goede A, Ter Braack E, van Putten M. Accurate coil positioning is important for single and paired pulse TMS on the subject level. Brain Topogr 2018;31(6):917–30.
[109] Harquel S, Bacle T, Beynel L, Marendaz C, Chauvin A, David O. Mapping dynamical properties of cortical microcircuits using robotized TMS and EEG: towards functional cytoarchitectonics. Neuroimage 2016;135:115–24.
[110] Goldenholz D, Ahlfors S, Hämäläinen M, Sharon D, Ishitobi M, Vaina L, et al. Mapping the signal-to-noise-ratios of cortical sources in magnetoencephalography and electroencephalography. Hum Brain Mapp 2009;30(4):1077–86.
[111] Hui J, Zomorrodi R, Lioumis P, Salavati B, Rajji TK, Chen R, et al. Pharmacological mechanisms of interhemispheric signal propagation: a TMS-EEG study. Neuropsychopharmacology 2020;45(6):932–9.
[112] Bertazzoli G, Esposito R, Mutanen T, Ferrari C, Ilmoniemi R, Miniussi C, et al. The impact of artifact removal approaches on TMS–EEG signal. Neuroimage 2021;239(118272):1–15.
[113] Rosanova M, Casarotto S, Pigorini A, Canali P, Casali AG, Massimini M. Combining transcranial magnetic stimulation with electroencephalography to study human cortical excitability and effective connectivity. Neuronal Network Anal: Concepts and Experiment Approach 2012;67:435–57.
[114] Komssi S, Huttunen J, Aronen H, Ilmoniemi R. EEG minimum-norm estimation compared with MEG dipole fitting in the localization of somatosensory sources at S1. Clin Neurophysiol 2004;115(3):534–42.
[115] VanRullen R. How to evaluate phase differences between trial groups in ongoing electrophysiological signals. Front Neurosci 2016;10(426):1–22.
[116] Schaworonkow N, Caldana Gordon P, Belardinelli P, Ziemann U, Bergmann T, Zrenner C. μ-Rhythm extracted with personalized EEG filters correlates with corticospinal excitability in real-time phase-triggered EEG-TMS. Front Neurosci 2018;12(954):1–6.
[117] Rossini P, Barker A, Berardelli A, Caramia M, Caruso G, Cracco R, et al. Non-invasive electrical and magnetic stimulation of the brain, spinal cord and roots: basic principles and procedures for routine clinical application. Report of an IFCN committee. Electroencephalogr Clin Neurophysiol 1994;91(2):79–92.
[118] Rothwell J, Hallett M, Berardelli A, Eisen A, Rossini P, Paulus W. Magnetic stimulation: motor evoked potentials. The international federation of clinical neurophysiology. Electroencephalogr Clin Neurophysiol Suppl 1999;52:97–103.
[119] Reijonen J, Pitkänen M, Kallioniemi E, Mohammadi A, Ilmoniemi R, Julkunen P. Spatial extent of cortical motor hotspot in navigated transcranial magnetic stimulation. J Neurosci Methods 2020;346(108893):1–9.
[120] Julkunen P, Säisänen L, Hukkanen T, Danner N, Könönen M. Does second-scale intertrial interval affect motor evoked potentials induced by single-pulse transcranial magnetic stimulation? Brain Stimul 2012;5(4):526–32.
[121] Pellicciari M, Miniussi C, Ferrari C, Koch G, Bortoletto M. Ongoing cumulative effects of single TMS pulses on corticospinal excitability: an intra- and inter-block investigation. Clin Neurophysiol 2016;127(1):621–8.
[122] Hassanzahraee M, Zoghi M, Jaberzadeh S. Longer transcranial magnetic stimulation intertrial interval increases size, reduces variability, and improves the reliability of motor evoked potentials. Brain Connect 2019;9(10):770–6.
[123] Pitkänen M, Kallioniemi E, Julkunen P. Effect of inter-train interval on the induction of repetition suppression of motor-evoked potentials using transcranial magnetic stimulation. PLoS One 2017;12(7):1–10.
[124] Tran D, McNair N, Harris J, Livesey E. Expected TMS excites the motor system less effectively than unexpected stimulation. Neuroimage 2021;226(117541):1–10.
[125] Awiszus F. Fast estimation of transcranial magnetic stimulation motor threshold: is it safe? Brain Stimul 2011;4(1):58–9.
[126] Capozio A, Chakrabarty S, Astill S. The effect of sound and stimulus expectation on transcranial magnetic stimulation-elicited motor evoked potentials. Brain Topogr 2021;34(6):720–30.
[127] Brown KE, Lohse KR, Mayer IMS, Strigaro G, Desikan M, Casula EP, et al. The reliability of commonly used electrophysiology measures. Brain Stimul 2017;10(6):1102–11.
[128] Stewart L, Walsh V, Rothwell J. Motor and phosphene thresholds: a transcranial magnetic stimulation correlation study. Neuropschologia 2001;39(4):415–9.

[129] Deblieck C, Thompson B, Iacoboni M, Wu AD. Correlation between motor and phosphene thresholds: a transcranial magnetic stimulation study. Hum Brain Mapp 2008;29(6):662–70.
[130] Stokes M, Chambers C, Gould I, Henderson T, Janko N, Allen N, et al. Simple metric for scaling motor threshold based on scalp-cortex distance: application to studies using transcranial magnetic stimulation. J Neurophysiol 2005;94(6):4520–7.
[131] Westin G, Bassi B, Lisanby S, Luber B. Determination of motor threshold using visual observation overestimates transcranial magnetic stimulation dosage: safety implications. Clin Neurophysiol 2014;125(1):142–7.
[132] Kammer T, Puls K, Strasburger H, Hill N, Wichmann F. Transcranial magnetic stimulation in the visual system. I. The psychophysics of visual suppression. Exp Brain Res 2005;160(1):118–28.
[133] Kammer T, Puls K, Erb M, Grodd W. Transcranial magnetic stimulation in the visual system. II. Characterization of induced phosphenes and scotomas. Exp Brain Res 2005;160(1):129–40.
[134] Taylor P, Walsh V, Eimer M. The neural signature of phosphene perception. Hum Brain Mapp 2010;31(9):1408–17.
[135] Marg E, Rudiak D. Phosphenes induced by magnetic stimulation over the occipital brain: description and probable site of stimulation. Optom Vis Sci 1994;71(5):301–11.
[136] Antal A, Nitsche M, Kincses T, Lampe C, Paulus W. No correlation between moving phosphene and motor thresholds: a transcranial magnetic stimulation study. Neuroreport 2004;15(2):297–302.
[137] Romei V, Gross J, Thut G. On the role of prestimulus alpha rhythms over occipito-parietal areas in visual input regulation: correlation or causation? J Neurosci 2010;30(25):8692–7.
[138] Zazio A, Bortoletto M, Ruzzoli M, Miniussi C, Veniero D. Perceptual and physiological consequences of dark adaptation: a TMS-EEG study. Brain Topogr 2019;32(5):773–82.
[139] Janssen A, Oostendorp T, Stegeman D. The coil orientation dependency of the electric field induced by TMS for M1 and other brain areas. J NeuroEng Rehabil 2015;12(47):1–13.
[140] Janssen A, Oostendorp T, Stegeman D. The effect of local anatomy on the electric field induced by TMS: evaluation at 14 different target sites. Med Biol Eng Comput 2014;52(10):873–83.
[141] Julkunen P, Saisanen L, Danner N, Awiszus F, Kononen M. Within-subject effect of coil-to-cortex distance on cortical electric field threshold and motor evoked potentials in transcranial magnetic stimulation. J Neurosci Methods 2012;206(2):158–64.
[142] Casali AG, Casarotto S, Rosanova M, Mariotti M, Massimini M. General indices to characterize the electrical response of the cerebral cortex to TMS. Neuroimage 2010;49(2):1459–68.
[143] Kähkönen S, Wilenius J, Komssi S, Ilmoniemi R. Distinct differences in cortical reactivity of motor and prefrontal cortices to magnetic stimulation. Clin Neurophysiol 2004;115(3):583–8.
[144] Komssi S, Savolainen P, Heiskala J, Kähkönen S. Excitation threshold of the motor cortex estimated with transcranial magnetic stimulation electroencephalography. Neuroreport 2007;18(1):13–6.
[145] Raffin E, Harquel S, Passera B, Chauvin A, Bougerol T, David O. Probing regional cortical excitability via input-output properties using transcranial magnetic stimulation and electroencephalography coupling. Hum Brain Mapp 2020;41(10):2741–61.
[146] Schaworonkow N, Triesch J, Ziemann U, Zrenner C. EEG-triggered TMS reveals stronger brain state-dependent modulation of motor evoked potentials at weaker stimulation intensities. Brain Stimul 2019;12(1):110–8.
[147] Zmeykina E, Mittner M, Paulus W, Turi Z. Weak rTMS-induced electric fields produce neural entrainment in humans. Sci Rep 2020;10(1):1–16. 11994.
[148] Kähkönen S, Komssi S, Wilenius J, Ilmoniemi R. Prefrontal transcranial magnetic stimulation produces intensity-dependent EEG responses in humans. Neuroimage 2005;24(4):955–60.
[149] Muggleton NG, Juan CH, Cowey A, Walsh V. Human frontal eye fields and visual search. J Neurophysiol 2003;89(6):3340–3.
[150] O'Shea J, Muggleton NG, Cowey A, Walsh V. Timing of target discrimination in human frontal eye fields. J Cognit Neurosci 2004;16(6):1060–7.
[151] Juan CH, Muggleton NG, Tzeng OJ, Hung DL, Cowey A, Walsh V. Segregation of visual selection and saccades in human frontal eye fields. Cerebr Cortex 2008;18(10):2410–5.
[152] Silvanto J, Lavie N, Walsh V. Stimulation of the human frontal eye fields modulates sensitivity of extrastriate visual cortex. J Neurophysiol 2006;96(2):941–5.
[153] Voineskos A, Farzan F, Barr M, Lobaugh N, Mulsant B, Chen R, et al. The role of the corpus callosum in transcranial magnetic stimulation induced interhemispheric signal propagation. Biol Psychiatr 2010;68(9):825–31.
[154] Kallioniemi E, Könönen M, Julkunen P. Repeatability of functional anisotropy in navigated transcranial magnetic stimulation–coil-orientation versus response. Neuroreport 2015;26(9):515–21.
[155] Belardinelli P, Biabani M, Blumberger D, Bortoletto M, Casarotto S, David O, et al. Reproducibility in TMS-EEG studies: a call for data sharing, standard procedures and effective experimental control. Brain Stimul 2019;12(3):787–90.
[156] Conde V, Tomasevic L, Akopian I, Stanek K, Saturnino G, Thielscher A, et al. The non-transcranial TMS-evoked potential is an inherent source of ambiguity in TMS-EEG studies. Neuroimage 2019;85:300–12.
[157] Siebner H, Conde V, Tomasevic L, Thielscher A, Bergmann T. Distilling the essence of TMS-evoked EEG potentials (TEPs): a call for securing mechanistic specificity and experimental rigor. Brain Stimul 2019;12(4):1051–4.
[158] de Graaf T, Sack A. Null results in TMS: from absence of evidence to evidence of absence. Neurosci Biobehav Rev 2011;35(3):871–7.
[159] Russo S, Sarasso S, Puglisi GE, Dal Palù D, Pigorini A, Casarotto S, et al. TAAC - TMS Adaptable Auditory Control: a universal tool to mask TMS clicks. J Neurosci Methods 2022;370:109491.
[160] Pellegrino G, Schuler AL, Arcara G, Di Pino G, Piccione F, Kobayashi E. Resting state network connectivity is attenuated by fMRI acoustic noise. Neuroimage 2022;247:118791.
[161] Sarasso S, D'Ambrosio S, Fecchio M, Casarotto S, Viganò A, Landi C, et al. Local sleep-like cortical reactivity in the awake brain after focal injury. Brain 2020;143(12):3672–84.
[162] ter Braack E, de Vos C, van Putten M. Masking the auditory evoked potential in TMS-EEG: a comparison of various methods. Brain Topogr 2015;28(3):520–8.
[163] Nikouline V, Ruohonen J, Ilmoniemi R. The role of the coil click in TMS assessed with simultaneous EEG. Clin Neurophysiol 1999;110(8):1325–8.
[164] Ohbayashi W, Kakigi R, Nakata H. Effects of white noise on event-related potentials in somatosensory Go/No-go paradigms. Neuroreport 2017;28(13):788–92.
[165] Koponen LM, Goetz SM, Tucci DL, Peterchev AV. Sound comparison of seven TMS coils at matched stimulation strength. Brain Stimul 2020;13(3):873–80.
[166] Ruohonen J, Ollikainen M, Nikouline V, Virtanen J, Ilmoniemi R. Coil design for real and sham transcranial magnetic stimulation. IEEE Trans Biomed Eng 2000;47(2):145–8.
[167] Gordon PC, Jovellar DB, Song Y, Zrenner C, Belardinelli P, Siebner HR, et al. Recording brain responses to TMS of primary motor cortex by EEG - utility of an optimized sham procedure. Neuroimage 2021;245:118708.
[168] Rossi S, Ferro M, Cincotta M, Ulivelli M, Bartalini S, Miniussi C, et al. A real electro-magnetic placebo (REMP) device for sham transcranial magnetic stimulation (TMS). Clin Neurophysiol 2007;118(3):709–16.
[169] Amaro Jr E, Barker GJ. Study design in fMRI: basic principles. Brain Cognit 2006;60(3):220–32.
[170] Premoli I, Castellanos N, Rivolta D, Belardinelli P, Bajo R, Zipser C, et al. TMS-EEG signatures of GABAergic neurotransmission in the human cortex. J Neurosci 2014;34(16):5603–12.
[171] Veniero D, Ponzo V, Koch G. Paired associative stimulation enforces the communication between interconnected areas. J Neurosci 2013;33(34):13773–83.
[172] Vernet M, Bashir S, Yoo W, Perez J, Najib U, Pascual-Leone A. Insights on the neural basis of motor plasticity induced by theta burst stimulation from TMS-EEG. Eur J Neurosci 2013;37(4):598–606.
[173] Leodori G, Fabbrini A, De Bartolo MI, Costanzo M, Asci F, Palma V, et al. Cortical mechanisms underlying variability in intermittent theta-burst stimulation-induced plasticity: a TMS-EEG study. Clin Neurophysiol 2021;132(10):2519–31.
[174] Rocchi L, Ibanez J, Benussi A, Hannah R, Rawji V, Casula E, et al. Variability and predictors of response to continuous theta burst stimulation: a TMS-EEG study. Front Neurosci 2018;12:400.
[175] Morishima Y, Akaishi R, Yamada Y, Okuda J, Toma K, Sakai K. Task-specific signal transmission from prefrontal cortex in visual selective attention. Nat Neurosci 2009;12(1):85–91.
[176] Meteyard L, Holmes N. Tms smart - scalp mapping of annoyance ratings and twitches caused by Transcranial Magnetic Stimulation. J Neurosci Methods 2018;299:34–44.
[177] Bergmann T. Brain state-dependent brain stimulation. Front Psychol 2018;9(2108):1–4.
[178] Karabanov A, Thielscher A, Siebner HR. Transcranial brain stimulation: closing the loop between brain and stimulation. Curr Opin Neurol 2016;29(4):397–404.
[179] Esposito R, Bortoletto M, Miniussi C. Integrating TMS, EEG, and MRI as an approach for studying brain connectivity. Neuroscientist 2020;26(5–6):471–86.
[180] Bergmann TO, Lieb A, Zrenner C, Ziemann U. Pulsed facilitation of corticospinal excitability by the sensorimotor mu-alpha rhythm. J Neurosci 2019;39(50):10034–43.
[181] Zrenner C, Desideri D, Belardinelli P, Ziemann U. Real-time EEG-defined excitability states determine efficacy of TMS-induced plasticity in human motor cortex. Brain Stimul 2018;11(2):374–89.
[182] Karabanov AN, Madsen KH, Krohne LG, Siebner HR. Does pericentral mu-rhythm "power" corticomotor excitability? - a matter of EEG perspective. Brain Stimul 2021;14(3):713–22.
[183] Madsen KH, Karabanov AN, Krohne LG, Safeldt MG, Tomasevic L, Siebner HR. No trace of phase: corticomotor excitability is not tuned by phase of pericentral mu-rhythm. Brain Stimul 2019;12(5):1261–70.
[184] Bergmann TO, Born J. Phase-amplitude coupling: a general mechanism for memory processing and synaptic plasticity? Neuron 2018;97(1):10–3.
[185] Schaworonkow N, Nikulin VV. Is sensor space analysis good enough? Spatial patterns as a tool for assessing spatial mixing of EEG/MEG rhythms. Neuroimage 2022;253:119093.
[186] Ilmoniemi RJ, Hernandez-Pavon JC, Makela NN, Metsomaa J, Mutanen TP, Stenroos M, et al. Dealing with artifacts in TMS-evoked EEG. Conf Proc IEEE Eng Med Biol Soc 2015;2015:230–3.

[187] Rogasch N, Sullivan C, Thomson R, Rose N, Bailey N, Fitzgerald P, et al. Analysing concurrent transcranial magnetic stimulation and electroencephalographic data: a review and introduction to the open-source TESA software. Neuroimage 2017;147:934–51.
[188] Vernet M, Thut G. Electroencephalography during transcranial magnetic stimulation: current modus operandi. In: Rotenberg A, Horvath J, Pascual-Leone A, editors. Transcranial magnetic stimulation. Neuromethods. New York, NY: Humana Press; 2014.
[189] Litvak V, Komssi S, Scherg M, Hoechstetter K, Classen J, Zaaroor M, et al. Artifact correction and source analysis of early electroencephalographic responses evoked by transcranial magnetic stimulation over primary motor cortex. Neuroimage 2007;37(1):56–70.
[190] Julkunen P, Pääkkönen A, Hukkanen T, Könönen M, Tiihonen P, Vanhatalo S, et al. Efficient reduction of stimulus artefact in TMS-EEG by epithelial short-circuiting by mini-punctures. Clin Neurophysiol 2008;119(2):475–81.
[191] Picton T, Hillyard S. Cephalic skin potentials in electroencephalography. Electroencephalogr Clin Neurophysiol 1972;33(4):419–24.
[192] Johnson J. Thermal agitation of electricity in conductors. Nature 1927;119:50–1.
[193] Nyquist H. Thermal agitation of electric charge in conductors. Phys Rev 1928;(32):110–3.
[194] Burbank D, Webster J. Reducing skin potential motion artefact by skin abrasion. Med Biol Eng Comput 1978;16(1):31–8.
[195] Li B, Virtanen J, Oeltermann A, Schwarz C, Giese M, Ziemann U, et al. Lifting the veil on the dynamics of neuronal activities evoked by transcranial magnetic stimulation. Elife 2017;6(e30552):1–22.
[196] de Talhouet H, Webster J. The origin of skin-stretch-caused motion artifacts under electrodes. Physiol Meas 1996;17(2):81–93.
[197] Ruddy K, Woolley D, Mantini D, Balsters J, Enz N, Wenderoth N. Improving the quality of combined EEG-TMS neural recordings: introducing the coil spacer. J Neurosci Methods 2018;294:34–9.
[198] Berg P, Scherg M. Dipole models of eye movements and blinks. Electroencephalogr Clin Neurophysiol 1991;79(1):36–44.
[199] Lins O, Picton T, Berg P, Scherg M. Ocular artifacts in recording EEGs and event-related potentials. II: source dipoles and source components. Brain Topogr 1993;6(1):65–78.
[200] Korhonen RJ, Hernandez-Pavon JC, Metsomaa J, Mäki H, Ilmoniemi RJ, Sarvas J. Removal of large muscle artifacts from transcranial magnetic stimulation-evoked EEG by independent component analysis. Med Biol Eng Comput 2011;49(4):397–407.
[201] Paus T, Sipila P, Strafella A. Synchronization of neuronal activity in the human primary motor cortex by transcranial magnetic stimulation: an EEG study. J Neurophysiol 2001;86(4):1983–90.
[202] Friedman B, Thayer J. Facial muscle activity and EEG recordings: redundancy analysis. Electroencephalogr Clin Neurophysiol 1991;79(5):358–60.
[203] Hernandez-Pavon JC, Metsomaa J, Mutanen T, Stenroos M, Mäki H, Ilmoniemi RJ, et al. Uncovering neural independent components from highly artifactual TMS-evoked EEG data. J Neurosci Methods 2012;209(1):144–57.
[204] Tiitinen H, Virtanen J, Ilmoniemi R, Kamppuri J, Ollikainen M, Ruohonen J, et al. Separation of contamination caused by coil clicks from responses elicited by transcranial magnetic stimulation. Clin Neurophysiol 1999;110(5):982–5.
[205] Ross JM, Sarkar M, Keller CJ. Experimental suppression of transcranial magnetic stimulation-electroencephalography sensory potentials. Hum Brain Mapp 2022;43(17):5141–53.
[206] Massimini M, Ferrarelli F, Esser SK, Riedner BA, Huber R, Murphy M, et al. Triggering sleep slow waves by transcranial magnetic stimulation. Proc Natl Acad Sci U S A 2007;104(20):8496–501.
[207] Mizukami H, Kakigi R, Nakata H. Effects of stimulus intensity and auditory white noise on human somatosensory cognitive processing: a study using event-related potentials. Exp Brain Res 2019;237(2):521–30.
[208] Koponen LM, Goetz SM, Peterchev AV. Double-containment coil with enhanced winding mounting for transcranial magnetic stimulation with reduced acoustic noise. IEEE Trans Biomed Eng 2021;68(7):2233–40.
[209] Gordon P, Desideri D, Belardinelli P, Zrenner C, Ziemann U. Comparison of cortical EEG responses to realistic sham versus real TMS of human motor cortex. Brain Stimul 2018;11(6):1322–30.
[210] Kappenman ES, Luck SJ. The effects of electrode impedance on data quality and statistical significance in ERP recordings. Psychophysiology 2010;47(5):888–904.
[211] de Cheveigné A, Nelken I. Filters: when, why, and how (not) to use them. Neuron 2019;102(2):280–93.
[212] de Cheveigné A, Arzounian D. Robust detrending, rereferencing, outlier detection, and inpainting for multichannel data. Neuroimage 2018;172:903–12.
[213] Hernandez-Pavon JC, Kugiumtzis D, Zrenner C, Kimiskidis VK, Metsomaa J. Removing artifacts from TMS-evoked EEG: A methods review and a unifying theoretical framework. J Neurosci Methods 2022;376:109591.
[214] Farrens J, Simmons A, Luck S, Kappenman E. Electroencephalogram (EEG) recording protocol for cognitive and affective human neuroscience research. Research Square 2020:1–24.
[215] Lioumis P, Zomorrodi R, Hadas I, Daskalakis ZJ, Blumberger DM. Combined transcranial magnetic stimulation and electroencephalography of the dorsolateral prefrontal cortex. JoVE 2018;138.
[216] Hassan U, Pillen S, Zrenner C, Bergmann T. The Brain Electrophysiological recording & STimulation (BEST) toolbox. Brain Stimul 2022;15(1):109–15.
[217] Sekiguchi H, Takeuchi S, Kadota H, Kohno Y, Nakajima Y. TMS-induced artifacts on EEG can be reduced by rearrangement of the electrode's lead wire before recording. Clin Neurophysiol 2011;122(5):984–90.
[218] Mutanen T, Kukkonen M, Nieminen J, Stenroos M, Sarvas J, Ilmoniemi R. Recovering TMS-evoked EEG responses masked by muscle artifacts. Neuroimage 2016;139:157–66.
[219] Nunez PL, Srinivasan R. Electric fields of the brain: the neurophysics of EEG. Oxford University Press; 2006.
[220] Rogasch NC, Biabani M, Mutanen TP. Designing and comparing cleaning pipelines for TMS-EEG data: a theoretical overview and practical example. J Neurosci Methods 2022;371:109494.
[221] Mutanen T, Metsomaa J, Liljander S, Ilmoniemi R. Automatic and robust noise suppression in EEG and MEG: the SOUND algorithm. Neuroimage 2018;166:135–51.
[222] Ross JM, Ozdemir RA, Lian SJ, Fried PJ, Schmitt EM, Inouye SK, et al. A structured ICA-based process for removing auditory evoked potentials. Sci Rep 2022;12(1):1391.
[223] Biabani M, Fornito A, Mutanen T, Morrow J, Rogasch N. Characterizing and minimizing the contribution of sensory inputs to TMS-evoked potentials. Brain Stimul 2019;12(6):1537–52.
[224] Nieminen JO, Gosseries O, Massimini M, Saad E, Sheldon AD, Boly M, et al. Consciousness and cortical responsiveness: a within-state study during non-rapid eye movement sleep. Sci Rep 2016;6:30932.
[225] Onton J, Westerfield M, Townsend J, Makeig S. Imaging human EEG dynamics using independent component analysis. Neurosci Biobehav Rev 2006;30(6):808–22.
[226] Bell A, Sejnowski T. An information-maximization approach to blind separation and blind deconvolution. Neural Comput 1995;7(6):1129–59.
[227] Hyvärinen A, Oja E. Independent component analysis: algorithms and applications. Neural Network 2000;13(4–5):411–30.
[228] Iwahashi M, Arimatsu T, Ueno S, Iramina K. Differences in evoked EEG by transcranial magnetic stimulation at various stimulus points on the head. Conf Proc IEEE Eng Med Biol Soc 2008;2008:2570–3.
[229] Hamidi M, Slagter H, Tononi G, Postle B. Brain responses evoked by high-frequency repetitive transcranial magnetic stimulation: an event-related potential study. Brain Stimul 2010;3(1):2–14.
[230] Jolliffe I. Principal component analysis. second ed. Springer; 2002.
[231] ter Braack E, de Jonge B, van Putten M. Reduction of TMS induced artifacts in EEG using principal component analysis. IEEE Trans Neural Syst Rehabil Eng 2013;21:376–82.
[232] Guzmán López J, Hernandez-Pavon JC, Lioumis P, Mäkelä JP, Silvanto J. State-dependent TMS effects in the visual cortex after visual adaptation: a combined TMS–EEG study. Clin Neurophysiol 2021;134:129–36.
[233] Uusitalo M, Ilmoniemi R. Signal-space projection method for separating MEG or EEG into components. Med Biol Eng Comput 1997;35(2):135–40.
[234] Mäki H, Ilmoniemi R. Projecting out muscle artifacts from TMS-evoked EEG. Neuroimage 2011;54(4):2706–10.
[235] Mutanen T, Biabani M, Sarvas J, Ilmoniemi R, Rogasch N. Source-based artifact-rejection techniques available in TESA, an open-source TMS-EEG toolbox. Brain Stimul 2020;13(5):1349–51.
[236] Saturnino G, Puonti O, Nielsen J, Antonenko D, Madsen K, Thielscher A. SimNIBS 2.1: a comprehensive pipeline for individualized electric field modelling for transcranial brain stimulation. In: Makarov S, Horner M, Noetscher G, editors. Brain and human body modeling: computational human modeling at EMBC 2018. Cham (CH): Springer; 2019.
[237] Stenroos M, Nummenmaa A. Incorporating and compensating cerebrospinal fluid in surface-based forward models of magneto- and electroencephalography. PLoS One 2016;11(7):1–23.
[238] Plonsey R, Heppner D. Considerations of quasi-stationarity in electrophysiological systems. Bull Math Biophys 1967;29(4):657–64.
[239] Makkonen M, Mutanen T, Metsomaa J, Zrenner C, Souza V, Ilmoniemi R. Real-time artifact detection and removal for closed-loop EEG-TMS. International Journal of Bioelectromagnetism 2021;23(2):1–4.
[240] Metsomaa J, Sarvas J, Ilmoniemi R. Multi-trial evoked EEG and independent component analysis. J Neurosci Methods 2014;228:15–26.
[241] Metsomaa J, Sarvas J, Ilmoniemi R. Blind source separation of event-related EEG/MEG. IEEE Trans Biomed Eng 2017;64(9):2054–64.
[242] Oostenveld R, Fries P, Maris E, Schoffelen J. FieldTrip: open source software for advanced analysis of MEG, EEG, and invasive electrophysiological data. Comput Intell Neurosci 2011;2011:156869.
[243] Atluri S, Frehlich M, Mei Y, Garcia Dominguez L, Rogasch N, Wong W, et al. TMSEEG: a MATLAB-based graphical user interface for processing electrophysiological signals during transcranial magnetic stimulation. Front Neural Circ 2016;10(78):1–20.

[244] Wu W, Keller C, Rogasch N, Longwell P, Shpigel E, Rolle C, et al. ARTIST: a fully automated artifact rejection algorithm for single-pulse TMS-EEG data. Hum Brain Mapp 2018;39(4):1607–25.
[245] Delorme A, Makeig S. EEGLAB: an open source toolbox for analysis of single-trial EEG dynamics including independent component analysis. J Neurosci Methods 2004;134(1):9–21.
[246] Habibollahi Saatlou F, Rogasch N, McNair N, Biabani M, Pillen S, Marshall T, et al. MAGIC: an open-source MATLAB toolbox for external control of transcranial magnetic stimulation devices. Brain Stimul 2018;11(5):1189–91.
[247] Gross J. Analytical methods and experimental approaches for electrophysiological studies of brain oscillations. J Neurosci Methods 2014;228(100):57–66.